PREDICTION OF BACKWATER LEVEL DUE TO BRIDGE CONSTRICTION IN WATERWAYS

by

Kimia Haji Amou Assar

A Thesis presented to the Faculty of the
American University of Sharjah
College of Engineering
In Partial Fulfillment
of the Requirements
for the Degree of

Master of Science in
Civil Engineering

Sharjah, United Arab Emirates

May 2019

Approval Signatures

We, the undersigned, approve the Master's Thesis of Kimia Haji Amou Assar.

Thesis Title: Prediction of the Backwater Level Due to Bridge Constriction in Waterways.

Signature **Date of Signature** (dd/mm/yyyy)

_____ _____

Dr. Serter Atabay
Professor, Department of Civil Engineering
Thesis Advisor

_____ _____

Dr. Md. Maruf Mortula
Professor, Department of Civil Engineering
Thesis Committee Member

_____ _____

Dr. Abdullah Gokhan Yilmaz
Assistant Professor, Department of Civil Engineering
University of Sharjah
Thesis Committee Member

_____ _____

Dr. Irtishad Ahmad
Head, Department of Civil Engineering

_____ _____

Dr. Lotfi Romdhane
Associate Dean for Graduate Affairs and Research
College of Engineering

_____ _____

Dr. Naif A. Darwish
Acting Dean, College of Engineering

_____ _____

Dr. Mohamed El-Tarhuni
Vice Provost for Graduate Studies

Acknowledgement

I am forever beholden to Dr. Serter Atabay, who has introduced me to the mesmerizing subject of water engineering, especially open channel hydraulics, when I was an undergraduate student at the American University of Sharjah. I would like to seize this opportunity to thank him for his dignified advices, patience, and motivation over the years that I have spent at the American University of Sharjah.

I am grateful to the professors of the Civil Engineering department at the American University of Sharjah who taught me during the bachelor and master programs. I also would like to thank American University of Sharjah for the graduate teaching assistantship I received during my master level studies.

I am most indebted to my parents, sister, grandparents, aunts, and cousins for all the love, happiness, support, and inspiration they have given me throughout my graduate studies and always.

Dedication

To my family, who raised me, supported me, educated me, and loved me…

Abstract

Worldwide, bridges and culverts built across rivers are obstacles to the flow which cause an increase in water depth at the upstream of the structure that significantly intensifies flooding of land and property upstream. Therefore, it is important to understand the effects of bridges and culverts on water levels for flood damage reduction, flood risk management, scour evaluation, flood risk mapping, and maintenance of rivers and channels. Moreover, the methods available in the literature are generally not convenient for engineers due to the complexity of the equations and procedures of each method. On the other hand, the simple methods available in the literature do not contain a high level of accuracy. Hence, acquiring a simple accurate empirical method for computing backwater is necessary. In this study, a series of parametric studies is conducted to examine the influence of different factors on backwater. The results of the parametric studies along with multiple regression analysis are used in deriving a simple accurate mathematical model for computing backwater. The proposed method is firstly compared with the most commonly used method, energy method, for different skew angles and roughness cases. The comparison of the results of the proposed and energy methods indicates high correlations between the two methods. Furthermore, the proposed method is validated by comparing its results with experimental data for normal (at 0º), and skewed crossings at 30º and 45º. The overall absolute average percentage difference between the proposed method and experimental data is found to be 5.1%, while the overall root-mean-square error is found to be 0.008. Thus, the empirical method proposed by this study is considered highly accurate as well as simple in comparison with available methods in the literature. Additionally, the proposed method is applicable for rectangular and arch bridges, multiple opening bridges, and any type of crossings (normal and skewed) in compound channels.

Keywords: ***Backwater; skewed crossings; compound channel; multiple openings; simple mathematical formula.***

Table of Contents

List of Figures

List of Tables

List of Abbreviations

ASOE	A single-opening semi-elliptical ARCH bridge
ASOSC	A single-opening semi-circular ARCH bridge
AMOSC	A multiple-opening semi-circular ARCH bridge
DECK	A single-opening straight deck bridges

Chapter 1. Introduction

This chapter embraces a short introduction about backwater due to bridge constrictions in waterways. In addition, the problem investigated in this study as well as the thesis contribution are presented. Conclusively, the general organization of the thesis is presented.

1.1. Overview

Bridge construction across waterways is considered to be entirely a challenge in civil engineering [1]. The constructed bridge across a river acts as an obstacle to the flow and narrows down the channel capacity; this phenomenon creates a head-loss which will be overcome by the increase of water level at the upstream of the bridge above the normal water level, that is called backwater. Consequently, it will become a challenge for hydraulic engineers to approve a bridge design assuring that the structure will not cause, or significantly intensify, flooding of land and property upstream [1].

As seen in Figure 1.1, the bridge causes an energy-loss due to flow contraction, friction between water and bridge surface, and flow expansion. The energy-loss increases the water surface at the upstream, which is known as backwater. Additionally, the increase of water level above the normal water at the upstream of the bridge is known as afflux, which is usually confused with head-loss. The majority of the energy loss is due to the expansion of the flow downstream of the bridge [3]. Furthermore, the degree of obstruction and an increase in flow rate result in an increase in backwater level.

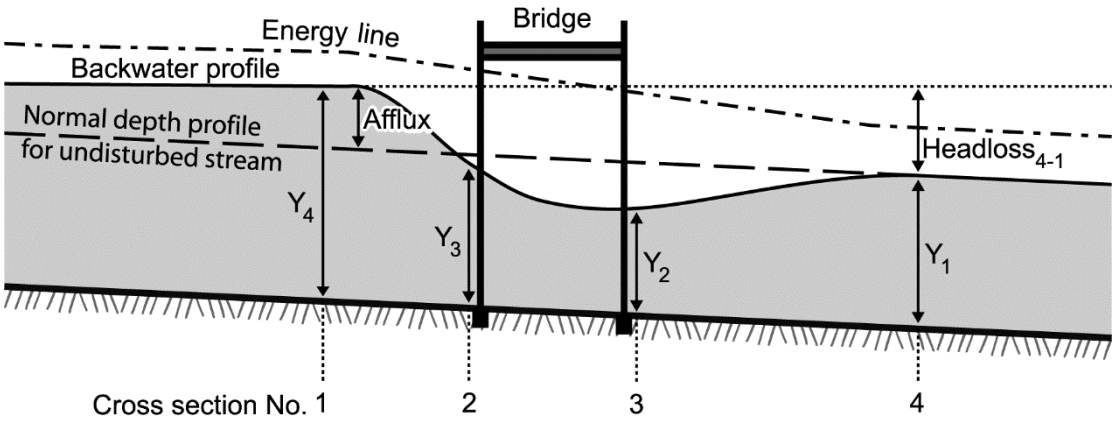

Figure 1.1: Side Elevation at a Bridge Constrictions [2].

Moreover, an ideal bridge spans over the entire waterway, and its deck is not reachable by the increasing flood level; however, this is not always the case. The span of the bridge, and the number and the shape of piers are dictated economically. In addition, some restrictions on the maximum level of the deck are applied due to the nature of the waterway and the site's geography. Hence, the design of the bridge turns out to be a complicated problem; it should take the hydraulics effects into consideration. Bridges should be designed in such a manner that guarantees that there will be no detrimental effect on the upstream properties due to the flood [1]. Thus, knowledge of bridge hydraulics is essential in order to avoid any flood situation when preparing for a new bridge design. The hydraulic investigation estimates the change in water levels caused by proposed or existing structure, which will help to improve the design to alleviate the problem [1]. Additionally, the hydraulic analysis is considered an important aspect of many activities such as flood damage reduction, flood risk mapping, scour evaluation, and maintenance of rivers and channels [2].

Furthermore, over the past several decades the problems associated with backwater at bridge constrictions have become the subject of a significant body of research, mainly due to their impact on upstream properties as well as the degree of economic disruption [4]. According to Bradley, regardless of the method implemented, analysis of bridge backwater is not straight forward [5]. The complexity of the equations and procedures of the available methods lead many researchers on to concentrate on developing simple mathematical methods for backwater computation. The benefit of mathematical methods is that once the data is entered, a range of scenarios can be investigated, and complex problems can be solved with the least amount of effort [6]. However, the proposed methods available in literature do not contain a high level of accuracy and can be only implemented for approximate backwater estimations. Hence, this study aims to acquire a simple mathematical formula with high accuracy for estimating backwater which considers different bridge opening shapes, multiple openings, and skewed crossings.

1.2. Thesis Objectives

Due to the importance of bridge backwater analysis, the complexity of available equations and procedures, and the lack of accuracy of the proposed methods in already existing literature, this study will focus on developing a simple mathematical method

for calculating backwater at bridge constrictions considering multiple openings and skewed bridges. In order to derive the simple mathematical formula, a series of parametric studies is conducted, especially on skewed bridges, exploring the factors affecting backwater level.

1.3. Research Contribution

The contributions of this research work can be summarized as follows:

- Definition of the best traditional bridge modeling approaches available in literature
- An investigation of the factors impacting backwater through the conduction of parametric studies
- Proposing a simple mathematical formula for computing backwater at bridge constrictions

1.4. Thesis Organization

The rest of the thesis is organized as follows: Chapter 2 presents the background information regarding bridge constriction as well as the work done in available literature on backwater. The computer modelling along with analysis and deriving the empirical formula procedures are discussed in Chapter 3. Chapter 4 presents the parametric studies in addition to the development of the mathematical formula. Chapter 5 presents the results of the proposed method and its comparison with energy method and experimental data. Conclusively, Chapter 6 concludes the thesis and outlines future work.

Chapter 2. Background and Literature Review

In this chapter, methods of calculating backwater, proposed simple methods, commercial software used in computing backwater, factors affecting the water levels, and the experimental data provided to be used in this study are discussed.

2.1. Conventional Methods of Computing Backwater

Analysis of backwater at bridge constrictions has been carried out by many researchers since 1840 [1]. Many methods were developed to calculate the water surface profile using basic mathematical and engineering concepts. The six methods mentioned in this section use the standard step method and the direct method (pseudo-time stepping method); the standard step method is based on energy equation, while the direct method is mainly based on numerical solutions of Saint Venant equations [4]. Moreover, the methods described in this section are referred to as conventional methods as they are already implemented within different software (HECRAS and InfoWorks).

2.1.1. Energy method. The energy method is considered as one of the most accurate approaches to computing backwater [2, 4], as it is capable of producing accurate estimates of water surface levels in waterways. It uses the Bernoulli's equation with inclusion of parameters to calculate backwater. The energy method is a multi-step procedure applied to all reaches between any two sequential cross-sections, beginning at cross-sections 1 and moving upstream to cross-section 4, as shown in Figure 1.1 [7]. Cross-section 1 and 4 determine the beginning of the contraction and the end of expansion, respectively [1]. In addition to the four cross-sections, BD (bridge downstream) and BU (bridge upstream) sections are generated inside the bridge structure to compute backwater. The energy equation is as follows:

$$h_{wsu} + \alpha_u \frac{V_u^2}{2g} = h_{wsd} + \alpha_d \frac{V_d^2}{2g} + LS_f + C \left| \alpha_u \frac{V_u^2}{2g} - \alpha_d \frac{V_d^2}{2g} \right| \quad (1)$$

Where:

h_{wsu} = water surface elevation at the upstream

h_{wsd} = water surface elevation at the downstream

V_u = velocity at upstream

V_d = velocity at downstream

α_u = velocity distribution coefficient for kinetic energy at the upstream

α_d = velocity distribution coefficient for kinetic energy at the downstream

g = gravitational acceleration

L = reach length

C = contraction/expansion coefficient

S_f = reach-averaged friction slope

2.1.2. Momentum method. The basic principle in this method is to perform a momentum balance in the area where the flow is disturbed. Similar to the energy method, the momentum method is also applied from downstream to upstream over several steps [1]. The momentum equation used for the calculation of backwater is shown in the equation below:

$$A_u\bar{Y}_u + \frac{\beta_u Q_u^2}{gA_u} = A_d\bar{Y}_d - A_{Pd}\bar{Y}_{Pd} + \frac{\beta_d Q_d^2}{gA_d} + F_f - W_x \quad (2)$$

Where:

A_u = active flow area at upstream cross-section

A_{pd} = obstructed area of the pier on the downstream side

A_d = active flow area at downstream cross-section

$\bar{Y}_u$ = the vertical distance from the water surface to center of gravity of flow area A_u

$\bar{Y}_{pd}$ = the vertical distance from water surface to center of gravity of wetted pier area on downstream side

$\bar{Y}_d$ = the vertical distance from the water surface to center of gravity of flow area A_d

β_u = the velocity weighting coefficient at section upstream

β_d = the velocity weighting coefficient at downstream cross-section

Q_u = the discharge at section upstream

Q_d = the discharge at downstream cross-section

F_f = external force due to friction per unit weight of water

W_x = the force due to weight of water in the direction of flow per unit weight of water

2.1.3. Yarnell's method. Between 1927 and 1931 Yarnell conducted about 2600 experiments on the obstructive effect of bridges piers to the water flow. He

published his work in 1934 in which he evaluated the effects of the followings on water surface elevations [1]:

- The shape of the pier nose
- The shape of pier tail
- The channel contraction caused by the pier
- The length of the pier
- The angle between the longitudinal centerline of the pier and the approaching water stream (skew angle ϕ)
- The quantity of flow

Based on the studies conducted Yarnell's method was proposed [8]. This method predicts the change in water surface between the two regions after and before the bridge from downstream to upstream [4], [8]. The equation is as follows:

$$H_{2-3} = 2K(K + 10\omega - 0.6)(\alpha + 15\alpha^4)\frac{V_2^2}{2g} \quad (3)$$

Where:

$H_{3\text{-}2}$ = drop in water surface elevation from section 3 to 2

K = Yarnell's pier shape coefficient

ω = ratio of velocity head to depth at section 2

α = obstructed area of the piers divided by the total unobstructed area at section 2

V_2 = velocity downstream at section

2.1.4. Water Surface Profile method (WSPRO). The WSPRO model was developed by Shearman et al. to compute the water surface profile through a bridge based upon the definition of a minimum of four cross sections. This model mainly uses the basic energy equation [4, 9]. The WSPRO uses a procedure developed by Schnider et al. for analyzing bridge backwater under free-surface flow conditions [10]. The sequences of calculation go from downstream to upstream which is represented below:

$$h_4 + \alpha_4\frac{V_4^2}{2g} = h_1 + \alpha_1\frac{V_1^2}{2g} + h_L(4-1) \quad (4)$$

Where:

h_1 = water surface elevation at section 1

V_1 = velocity at section 1

h_4 = water surface elevation at section 4

V_4 = velocity at section 4

$h_{L(4-1)}$ = energy losses from section 4 to 1

2.1.5. Arch bridge method. The arch bridge method demonstrates the dependency of the backwater and related energy loss on the drag characteristics of smooth circular cylinders [4, 11]. The main relationship in this method is represented by a graph relating the ratio of backwater to downstream depth (dh/D_1) with the downstream Froude number (F_1), plotted for different downstream blockage ratios (J_1) [2]. The theoretical approach for this method leads to the following equations:

$$\left(\frac{dh}{D_3}\right)^3 = 3\left(\frac{dh}{D_3}\right)^2 + 2\left(\frac{dh}{D_3}\right) - 2(F_3)^2\left(\frac{dh}{D_3}\right) - CD \times J_1 \times (F_3)^2 = 0 \quad (5)$$

$$\left(\frac{dh}{D_3}\right)^3 = 3\left(\frac{dh}{D_3}\right)^2 + 2\left(\frac{dh}{D_3}\right) - 2(F_3)^2\left(\frac{dh}{D_3}\right) - \left(\frac{CD \times J_1 \times (F_3)^2}{\frac{dh}{D_3}+1}\right) = 0 \quad (6)$$

Where:

dh = backwater term (D_1-D_3)

D_1 = upstream depth of flow

D_3 = downstream depth of flow

F_3 = Froude number at depth D_3

J_1 = upstream blockage ratio (area of blockage of bridge at depth D_1/area of flow)

J_3 = downstream blockage ratio (area of blockage of bridge at depth D_3/area of flow)

CD = drag coefficient

2.1.6. US Bureau of Public Roads method (USBPR). The United States Bureau of Public Roads Method (USBPR) method is based on observations and studies made at a number of bridges at the United States [12]. The backwater equation used in this method is generated by applying the principle of conservation of energy between the point of maximum backwater (upstream from the bridge) and the point at the downstream [2, 5]. The strength of this method is that it uses normal depth, which is often the only parameter that can be easily calculated; however, in order for the method

to be accurate, the site conditions should resemble those in the laboratory [1]. This method is also known as the modified Bradley method which is represented by Eq. 7.

$$dh = K^* \times \alpha_2 \frac{V_B^2}{2g} + \alpha_1 \left[\left(\frac{A_B}{A_4} \right)^2 - \left(\frac{A_B}{A_1} \right)^2 \right] \frac{V_B^2}{2g} \quad (7)$$

Where:

dh = the total backwater

K^* = the total backwater coefficient

α_1 = the kinetic energy coefficient at the upstream section

α_2 = the kinetic energy coefficient in the constriction

V_B = the average velocity in constriction

A_B = the gross water area in constriction

A_4 = the water area in downstream section

A_1 = the total water area in up-stream section including that produced by the backwater

2.2. Simple Methods of Computing Backwater Available in the Literature

Due to complexity of equations and procedures of the conventional backwater computational methods, many researchers have proposed mathematical methods to calculate backwater over the past decades. In this section, in addition to one-dimensional models, a two-dimensional numerical model is discussed; however, due to the complexity of the two-dimensional model this study focuses on developing a one-dimensional model. The methods discussed in this section are referred to as simple methods.

A numerical method for computing backwater called “contracted-opening” was proposed by Tracy and Carter based on laboratory data from the Georgia Institute of Technology for a rectangular channel at a given discharge. This method implements an approach section with a distance equal to the width of the bridge opening at the upstream and a constricted section located at the downstream. Conclusively, Tracy and Carter indicated that the water elevation at the downstream is not only influenced by the conditions at downstream end of the bridge, but also by the flow condition at the downstream [13]. Moreover, a study was conducted by Izzard in which the impact of the channel’s cross-sectional shape on the backwater level was explored by comparing a single rectangular channel and a compound channel. The study resulted in the

development of a simplified mathematical formula for backwater level computation; the simplified formula represents the relationship between the backwater ratio (Y_1/Y_n) and Froude number, which is shown in the equation below [14]:

$$\frac{Y_1}{Y_n} = 1 + 0.45\left(\frac{F}{M}\right)^2 \quad (8)$$

Where:

Y_1 = the total depth at the section of maximum backwater

Y_n = the normal flow depth of the channel with no constriction

F = the Froude number for uniform flow in the channel

M = the opening ratio, bridge opening width (b) to the channel opening width (B)

Similarly, a dimensional analysis based on a physical model of a rectangular channel, with an adjustable bed slope and a constriction normal to the flow, was conducted [12]. Experimental data was used to analyze the influence of different variables on backwater levels. The results of the analysis showed that if the normal depth and its Froude number are used, the impacts of channel slope and channel roughness are negligible. In addition, this study denoted the term 'opening ratio' for the ratio of the opening width to the channel width instead of the term 'contraction ratio'. Moreover, Liu et al. developed the following formula for calculating the backwater level at bridge constrictions in a prismatic channel [12]:

$$\left(\frac{Y_1}{Y_n}\right)^3 = 4.48F^2\left[\frac{1}{M} - \frac{2}{3}(25 - M)\right] + 1 \quad (9)$$

Where:

Y_1 = the total depth at the section of maximum backwater

Y_n = the normal flow depth of the channel with no constriction

F = the Froude number for uniform flow in the channel

M = the opening ratio; bridge opening width (b) to the channel opening width (B)

Moreover, research conducted by Biery and Delleur which mathematically proves that the opening ratio defined by Liu et al. [12] for rectangular opening bridges cannot be applied for arch opening bridges. Therefore, the study adjusted the opening ratio definition to the ratio of the normal depth cross-sectional area for the bridge

opening (A_{n2}) to the normal depth cross-sectional area for the channel (A_{n1}). Additionally, Biery and Delleur conducted studies on semicircular arch bridge constrictions; the study indicated the channel opening ratio as the factor governing in the prediction of backwater levels. Consequently, based on the experimental results of the studies conducted by Lie et al. [12], Eq. 10 was proposed by Biery and Delleur [15]. It should be noted that the Froude number used in Biery and Delleur method is for uniform flow in unconstricted channel and can be computed using Eq. 11.

$$\frac{Y_1}{Y_n} = 1 + 0.47\left(\frac{F}{M'}\right)^{2.26} \tag{10}$$

$$F = \frac{U}{\sqrt{g\left(\frac{Y_n}{\alpha}\right)}} \tag{11}$$

Where:

Y_1 = the total depth at the section of maximum backwater

Y_n = the normal flow depth of the channel with no constriction

F = the Froude number for uniform flow in the channel

M' = the modified opening ratio, A_{n2}/A_{n1}

U = the cross-sectional mean velocity

g = the gravitational acceleration

α = the kinetic energy correction factor, which was assumed to be 1.0

Similarly, a study was conducted by Kaatz and James investigated the performance and reliability of four methods of one-dimensional flow analysis of bridges, namely, the modified Bradley method, WSPRO, the HEC-2 normal bridge method, and the HEC-2 special bridge method [16]. The study was conducted based on field data provided in a publication by the US Army Corps of Engineers, which includes nine different bridge sites with thirteen flood events. The study concluded that while WSPRO overestimated the backwater levels, HEC-2 special bridge method and the modified Bradley method tended to underestimate the backwater levels. Analogously, the HEC-2 normal bridge method accurately computed the backwater level in the absence of a 4:1 expansion ratio. In other words, regardless of the huge input data requirement and modeling many finite elements, the two-dimensional models give a more practical results for the net backwater than the one-dimensional models [16].

In addition, Biglary and Strum conducted a series of experimental studies in which only rectangular opening bridges with compound cross-section and alluvial bed forms were used. The series of studies resulted in the derivation of a two-dimensional, depth-averaged, k-ε turbulence model for flow around bridge abutments which is represented by Eq. 12 [17]. For simplicity, the depth-average continuity, the transverse momentum, and k-ε turbulence equations are not represented in this study.

$$\frac{\partial(U\Omega)}{\partial X}+\frac{\partial(V\Omega)}{\partial Y}=\frac{\partial}{\partial X}\left[\Gamma\frac{\partial(\Omega)}{\partial X}\right]+\frac{\partial}{\partial Y}\left[\Gamma\frac{\partial(\Omega)}{\partial Y}\right]+S_{\Omega} \tag{12}$$

Where:

U = the longitudinal depth-averaged velocity

V = the transverse depth-averaged velocity

Ω = the depth-averaged continuity equation

Γ = the transverse momentum equation

S_{Ω} = the k-ε turbulence equation

Moreover, Seckin conducted a study based on previous experimental studies that addressed a compound channel with single semi-circular, multiple semi-circular, single elliptical, and straight deck bridge models with and without piers [4, 18, 19]. In this study, Seckin concludes that backwater level is highly dependent on the Froude number and the opening ratio for all bridge models. Moreover, based on several regression analyses, Seckin proposed a one-dimensional mathematical method which is represented by Eq. 13. The proposed formula was found to be more accurate than Izzard and Biery and Delleur methods [14, 15]; however, Seckin suggests that the method can be only applied in predesign stages due to its level of accuracy [19].

$$\frac{Y_1}{Y_n}=1+0.25\left(\frac{F}{M\prime}\right)^{1.98} \tag{13}$$

Where:

Y_1 = the total depth at the section of maximum backwater

Y_n = the normal flow depth of the channel with no constriction

F = the Froude number for uniform flow in the channel

M' = the modified opening ratio, A_{n2}/A_{n1} [15]

In continuation of Seckin study [19], Seckin took bridge crossings with two different skew angles into consideration. The study explores the influence of skewness

on bridges and suggests a quadratic equation for backwater computation. The proposed method is based on the relationship between Froude number, backwater ratio, and opening ratio, which is follows [20]:

$$\frac{Y_1}{Y_n} = aF^3 + bF^2 + cF \tag{14}$$

Where:

Y_1 = the total depth at the section of maximum backwater

Y_n = the normal flow depth of the channel with no constriction

F = the Froude number for uniform flow in the channel

a = $-56.244M^3+89.795M^2-47.378M+5.8345$

b = $62.744M^3-105.420M^2+53.061M-7.3290$

c = $-12.619M^3+25.476M^2-17.114M+3.9087$

M = the opening ratio

Additionally, in a study conducted by Seckin et al., two different skew angles were considered, and the numerical method of calculating drag coefficient was modified. The study noted that blockage ratio is as effective as the opening ratio and the Froude number; thus, it focused on improving the backwater prediction and suggested Eq. 15 as a new formula for computing backwater levels considering blockage ratio. Moreover, the proposed formula was then applied on US Geological Survey field data and was compared with the results of HEC-2 normal bridge method and WSPRO method. It was concluded that the proposed method is less accurate than WSPRO and HEC-2 methods; however, the level of accuracy was considered acceptable [21].

$$\frac{\Delta h}{h_3} = 3.6471(F_3 \times J_3)^{1.919} \tag{15}$$

Where:

Δh = afflux

h_3 = the downstream water depth

F_3 = the downstream Froude number

J_3 = the downstream blockage ratio; area of the bridge below the water level to the total flow area

Several studies available in the literature addressed the computation of backwater by implementing neural network (NN) techniques [22-25]. For instance, a study implemented an artificial neural network to compute backwater accurately. The adopted model uses main channel and floodplain Manning's roughness coefficients, bridge width, and discharge to compute backwater. The model was also used in order to conduct a series of parametric studies [22]. It should be noted that the neural network techniques are usually case by case based methods, so these techniques are not implemented in this study.

In a recent study, a simple mathematical formula was proposed based on a series of experimental data for single opening deck and arch bridges [4, 18, 21, 26]. The proposed formula was driven based on parametric studies conducted (which are explained in more details in Section 4.1. Parametric Studies on Skewed Crossings) and was validated using the experimental data and energy method. It was concluded that the proposed method corresponded well with the experimental data and the results obtained using the energy method. The proposed formula is shown by Eq. 16 [27]. However, this method is neglecting the skew angle, eccentricity, and multi-opening bridges and is only limited to low flow conditions.

$$\frac{Y_1}{Y_n} = 0.93 + \left[\frac{Q_{mc}}{Q_{tot}} \times \frac{b_{mc}}{b_{tot}} \left(\frac{F_{mc}}{M'}\right)^{\frac{Q_{tot}}{Q_{mc}}}\right] \quad (16)$$

Where:

Y_1 = the total depth at the section of maximum backwater

Y_n = the normal flow depth of the channel with no constriction

F_{mc} = the Froude number of the main channel

M' = The modified opening ratio [15]

Q_{mc} = the main channel discharge

Q_{tot} = the total discharge

b_{mc} = the main channel width

b_{tot} = the total channel width

2.3. Software Packages

There are several applications available for one-dimensional, two-dimensional, and three-dimensional water level predictions [28]. However, since this study focuses

on a one-dimensional analysis of water surface levels, only one-dimensional software packages are mentioned. The most commonly used software in the USA and the UK are HEC-RAS and InfoWorks, which are described below.

2.3.1. HEC-RAS. Hydrological Engineering Center's River Analysis System (HEC-RAS) is a one-dimensional analysis system that allows the performance of steady, unsteady flow hydraulics, sediment transport/mobile bed computations, and water temperature modeling. In addition to the four river analysis components, HEC-RAS includes hydraulic design features that can be applied on the computed basic water surface profiles. The two flow analysis components are explained briefly below [29]:

1) Steady Flow Water Surface Profiles: this component is used for calculating water surface profiles for a steady gradually varied flow which is capable of modeling subcritical, supercritical, and mixed flow regime water surface profiles. This component is designed for applications in flood plain management and flood insurance studies to evaluate floodway encroachments.

2) Unsteady Flow Simulation: it is used for simulation of unsteady flow data through a fully open channel network. The calculations for cross sections and hydraulic structures that are applied for steady flow data were integrated into the unsteady flow component. Furthermore, the unsteady flow component is implemented to model storage areas and hydraulic connections between storage areas as well as between stream reaches.

Furthermore, the variation in bridge routines included in HEC-RAS allows the analysis of a bridge using four different methods, energy method, momentum method, Yarnell's method, and WSPRO method, without the need of changing the bridge geometry [4].

2.3.2. InfoWorks. This software is a full hydrodynamic test system for demonstrating streams and levels in open channels and estuaries. InfoWorks flow covers both unsteady and steady flow solvers, with options that include simple backwater, flow routing, and full unsteady simulation. InfoWorks can demonstrate an extensive variety of hydraulic structures including every basic kind of bridges, sluices, culverts, pumps, and weirs [30]. The methods implemented in InfoWorks are Arch bridge method and the United State Bureau of Public Roads method (USBPR).

According to Atabay, in implementing the ARCH bridge and USBPR methods of InfoWorks, there is need for cross-checking the results assuring that they are accurate [2]. Hence, in this study, HEC-RAS commercial package will be used due to its higher accuracy in water surface calculations.

2.4. Factors Impacting Hydraulic Performance of the Bridge

This section includes the main factors that are affecting the hydraulic performance of a bridge across a waterway by covering their significance and illustrating their effects.

2.4.1. Depth of flow. Depending on the slope and geometry of the channel and the type of flow, the depth of flow (Y) can be calculated for a given discharge. The flow depth affects the values of Froude number, opening ratio, and conveyance as they are functions of the depth. Analogously, the hydraulic performance of the structure, as well as the type of flow at the structure, are associated with the flow depth. For instance, if the normal water level of an unconstricted channel is close to the height of the bridge deck, it is very likely that the constriction will be submerged [1].

2.4.2. The bridge opening ratio. The ratio of the flow passing straight through the bridge opening over the flow passing through the whole channel is called the bridge opening ratio (M) [1, 5, 13, 31, 32]; which is an assessment of the severity of constriction [1]. The bridge opening ratio can be calculated using the following equation:

$$M = \frac{q}{Q} \tag{17}$$

Where:

M = bridge opening ratio

q = discharge through a width (b)

Q = discharge through the full channel

Additionally, the bridge opening ratio is one of the most important factors in the calculation of backwater. Smaller bridge opening leads to a larger obstruction, the smaller the bridge opening ratio, and consequently the backwater will increase more [1]. The bridge opening ratio equation has been modified by many researchers in their proposed methods, which were discussed in the previous section.

2.4.3. Froude number. Froude number (*F*) is a dimensionless ratio of inertial to gravitational forces acting on the flow. It is an indication of the type of flow which affects the hydraulic behaviour of an open channel; for *F=1.0* the flow is critical, *F>1.0* the flow is supercritical, and *F<1.0* the flow is subcritical. Froude number equation is as follows [33]:

$$F = \frac{V}{\sqrt{gD}} \tag{18}$$

Where:

F = Froude number
V = average cross-sectional velocity
g = gravitational acceleration
D = hydraulic depth, flow area divided by top width

In open channel flow, Froude number affects the discharge through the bridge opening; as the value of Froude number increases the discharge increases and as a consequence, the backwater increases. In addition, Froude number is used as an indicator of where a backwater analysis should start [1].

2.4.4. Ratio of waterway length to span. The ratio of the waterway length between the upstream and downstream faces of the constriction (*L*) to the width of the constriction's opening (*b*) is defined as the ratio of waterway length to span (*L/b*). If *L/b<1.0,* the constriction is considered to be a bridge, and in case of *L/b>1.0,* the constriction is considered to be a culvert. According to Kindsvater and Carter [31], if the waterway length decreases, the discharge will be reduced across the waterway. Generally, longer waterways are known to be more efficient compared to short waterways; this is due to more controlled expansion and contraction along the longer waterways and hence a smaller energy-loss [1]. Therefore, the length ratio can affect the hydraulic performance of the bridge. The value for the length ratio can be simply calculated, and it will remain constant once the bridge is constructed.

2.4.5. Entrance rounding. Entrance rounding is another factor that affects the hydraulic performance of the constriction across the waterway. The hydraulic efficiency of a constriction increases as the entrance become rounder since the contraction of the waterway decreases [1].

2.4.6. Eccentricity. Eccentricity is referred to as the position of the bridge in relevance to the waterway channel. The quantity of eccentricity, e, can be computed as the ratio of the constriction width on the left floodplain (X_a) over the constriction width on the right floodplain (X_c); eccentricity impacts the contraction of the flow and as a consequence influences the hydraulic performance of the bridge [1]. In this study, eccentricity is not considered since all the data that are used to develop the simple model were collected using symmetrical bridge models.

2.4.7. Skew. The angle between the longitudinal centreline of the constriction and the waterway's channel bed, while the opening is parallel to the direction of the flow, is called skew angle (ϕ). There are four types of crossing which are:

- Normal crossing: the embankment is perpendicular to the flow, and the waterway is parallel to the flow ($\phi=0°$)
- Skew 1: the embankment is skewed to the flow, and the waterway is parallel to the flow
- Skew 2: both the embankment and the waterway are skewed to the flow
- Skew 3: the embankment is perpendicular to the flow, and the waterway is skewed to the flow

Moreover, among these crossing types, normal crossing and skew 1 and 2 are commonly occurring, while skew 3 is unusual. Skew angle has three impacts on hydraulic performance which are: the water levels at the two upstream corner of the channel vary, the effective width of the waterway is reduced which changes the opening ratio, and if the waterway is submerged, the flow emerging from the opening is angled towards one bank [1].

2.4.8. Shape of the waterway opening. The shape of constriction influences the distribution of velocity and flow pattern across the waterway. It also affects the coefficients of contraction and discharge [1].

2.4.9. Channel roughness and shape. Channel roughness and shape impact the hydraulic performance of a constriction indirectly. The channel roughness impacts the differential head across the opening, as the roughness increases the differential head increases. Furthermore, the channel shape and roughness affect the distribution of the discharge within the channel [1].

2.5. Available Experimental Data on Compound Channel

In this section, the procedure and experimental setup related to the experimental data provided for this study is explained. The experimental procedure and apparatus setup were discussed in details by Seckin and Atabay [4], Atabay and Knight [18], Seckin [19, 20], Seckin et al. [21], and Atabay [26]. Therefore, in this study the procedure and setup are explained briefly.Comprehensive laboratory experiments were carried out in two phases at the University of Birmingham, UK. In the first phase, a series of 145 experiments, 50 arch and 95 rectangular bridges were carried out. The experiments were performed on a non-tiling 22m long (with a test length of 18m), 1213mm wide, and 400mm deep flume. The flume was configured with a 398mm wide main channel and 407.3mm wide floodplains made of PVC material, which is shown in Figure 2.1. Three water circulation systems were implemented on the flume: two internal systems recirculating water from downstream end and one extended system passing water through the flume to the main laboratory sump. These systems include 50, 100, and 150mm pipelines; the discharge rates were measured by an electromagnetic flowmeter, a venturi-meter, and a Dull-tube respectively. Moreover, the depth-averaged velocity, U_d, were measured using a Novar-Nixon miniature propeller current meter for each discharge. There are four types of bridge openings that are modelled in these experiments: a single-opening semi-circular ARCH bridge (ASOSC), a single-opening semi-elliptical ARCH bridge (ASOE), a multiple-opening semi-circular ARCH bridge (AMOSC), and a single-opening straight deck bridges (DECK) with and without piers. Figure 2.2 represents different type of bridge openings implemented in the experimental study. Moreover, in natural waterways, floodplain roughness is different than the main channel; hence, in order to simulate the natural environment, aluminum wire grids with three different longitudinal intervals were placed along the flume. The intervals (λ) were 0.5, 0.25, and 0.125m for floodplain and 2.0, 3.0, and 4.0m for main channel. The aluminum meshes had an angle of 30º, height of 145mm, and width of 355mm. The roughness coefficients associated with this simulation are 0.022 to 0.136 for the floodplain and 0.025 to 0.039 for the main channel.

Figure 2.1: Experimental setup at Birmingham University, UK [4].

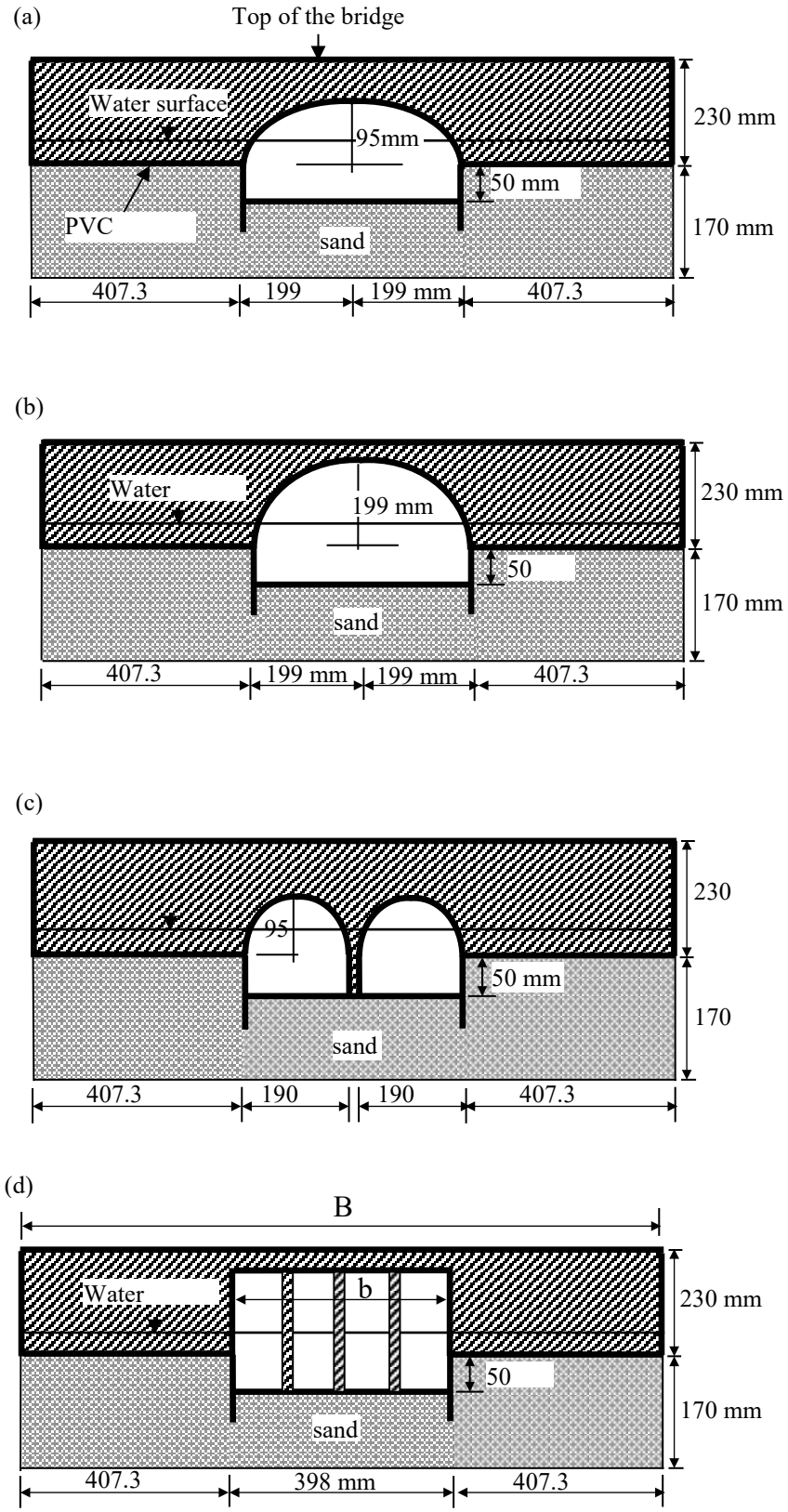

Figure 2.2: Cross-sections of bridge models used in this study: ASOE (a), ASOSC (b), AMOSC (c), DECK (d) [19].

Furthermore, water surface profiles were directly measured by pointer gauges for each discharge before and after adding the bridges. Initially, uniform flow condition was obtained by three adjustable tailgates downstream end of the flume; all the bridges were placed normal to the flow in the middle section of the flume in the first phase; and the bridges were placed as skewed crossings at ϕ=30º and ϕ=45º in the second phase with three Test cases A, B, and C. It should be noted that Test A and Test B represent Case 1 and 2 in the first phase, but Test C is a different condition Furthermore, in these experiments sluice gate flow, drowned orifice flow, and high flow conditions were ignored since the soffit of the bridges had no contact with the free surface flow. Additionally, Table 2.1 and

Table 2.2 represent different cases that were considered in both phases of experimental studies.

Table 2.1: Five cases considered in the first phase of experimental study.

Case No	Discharge (m^3/s)	Floodplain, *n*	Main Channel, *n*
1	0.010 & 0.055	0.010	0.009
2	0.015 & 0.050	0.022 & 0.050	0.009
3	0.015 & 0.035	0.040 & 0.061	0.025 & 0.036
4	0.015 & 0.040	0.054 & 0.094	0.023 & 0.039
5	0.021 & 0.035	0.092 & 0.136	0.026 & 0.039

Table 2.2: Three cases considered in the second phase of experimental study.

Test Case	Discharge (m^3/s)	Floodplain, *n*	Main Channel, *n*
A	0.018 & 0.040	0.010	0.009
B	0.018 & 0.040	0.022 & 0.050	0.009
C	0.018 & 0.040	0.014 & 0.016	0.017 & 0.025

Chapter 3. Methodology

In this chapter, the methodology adopted for this study to derive a simple mathematical formula is explained. First, a basic computer modelling with and without bridges is simulated on HEC-RAS. Then, a series of parametric studies is conducted from which the mathematical analysis is done in order to derive the formula. Lastly, the proposed method is evaluated and validated by implementing energy method and experimental data respectively. The details of each part of the methodology are presented below.

3.1. Computer Modelling

The experimental bridge models are simulated using HEC-RAS software package. The HEC-RAS models are firstly simulated under the low-flow condition without bridge to obtain the normal water surface level. Then, the models are simulated with bridge models of AMOSC, ASOE, and DECK having normal and skewed crossings. The skewed crossings are obtained using the built-in function in HEC-RAS, which readjusts the dimensions of the bridge model for the specified skew angle to define an equivalent cross-section perpendicular to the flow [29]. Due to the variation of roughness coefficients in the experimental data, the Manning's coefficients for the HEC-RAS models are set to range between 0.009 to 0.025 for the main channel and 0.010 to 0.016 for floodplain. The HEC-RAS model is embedded with cross-sections with a distance of 1.0m apart. Additionally, four extra cross-sections are placed as recommended by HEC-RAS manual [29, 34, 35]. As shown in Figure 3.1, the first cross-section is set at the upstream of the bridge at a distance equal to the bridge opening. The second and third cross-sections are placed immediately upstream and downstream of the bridge respectively. The last cross-section is placed at a distance of four times the opening of the bridge. The first and the last cross-sections represent the contraction and expansion lengths, with contraction and expansion coefficients substituted in the model; which are in this case 0.3 and 0.5 for contraction and expansion respectively. Additionally, Figure 3.2 represents an illustration of normal and skewed crossings.

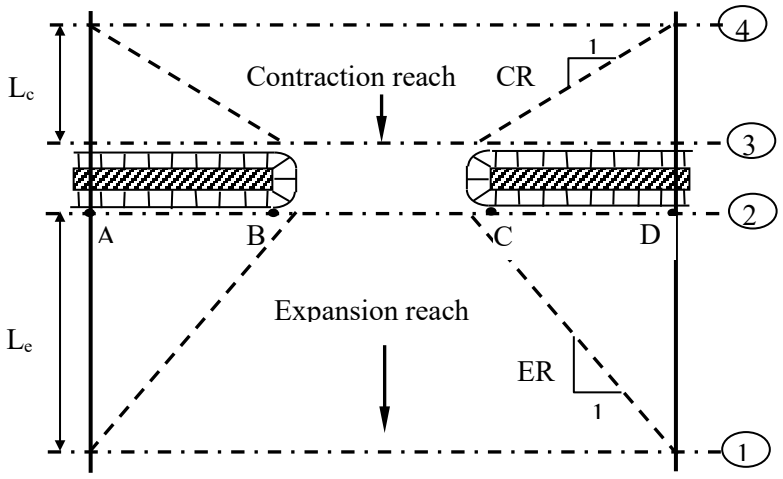

Figure 3.1: Plan of the flow through a bridge waterway specified by HEC-RAS [4, 29].

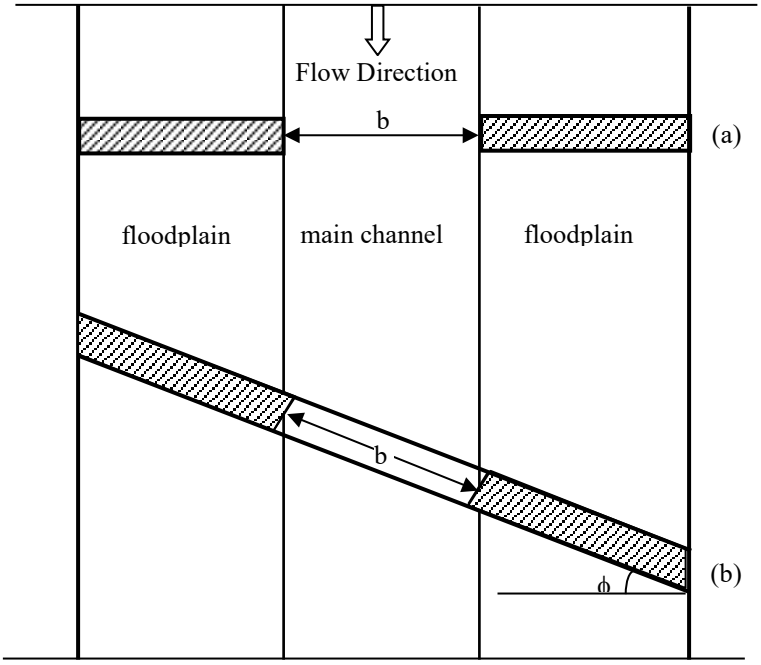

Figure 3.2: An illustration of different bridge crossings; (a) normal crossing (b) skewed crossing [20].

3.2. Analysis and Deriving the Formula

For developing a simple mathematical formula, a series of parametric studies are conducted, using the HEC-RAS bridge models, in order to find the impacts of different parameters on backwater levels such as roughness coefficient, flow, and skewness. The parametric studies are examined for a single opening straight deck

bridges (DECK) only with a bridge opening of 398mm. These studies include a variation of Manning's coefficients of 0.03 to 0.05 for the main channel (n_{mc}) and 0.05 to 0.07 for the floodplains (n_{fp}) with the increment of 0.005. In addition, the effects of different discharge values on backwater values are investigated by changing the discharge value from 15 l/s to 35 l/s with 5 l/s increments. Table 3.1 represents the values used in this parametric study; for all three cases, the skew angles of 0º, 5º, 10º, 15º, 20º, 25º, and 30º are used.

Table 3.1: Values for the parametric study.

Case 1		Case 2		Case 3		
n_{mc}	n_{fp}	n_{mc}	n_{fp}	n_{mc}	n_{fp}	*Q (l/s)*
0.030	0.050	0.030	0.050	0.030	0.050	15
0.035	0.050	0.030	0.055	0.030	0.050	20
0.040	0.050	0.030	0.060	0.030	0.050	25
0.045	0.050	0.030	0.065	0.030	0.050	30
0.050	0.050	0.030	0.070	0.030	0.050	35

A simple mathematical formula is proposed based on the results obtained from parametric studies. Since the mathematical analysis and parametric studies are major contributors in deriving the proposed method, Chapter 4 is dedicated to detailed discussions of these parts. Furthermore, the proposed method then is compared with the results of the energy method for adjustments. Lastly, the proposed method is compared with the experimental data to assure for its level of accuracy.

Chapter 4. Mathematical Analysis

As it was mentioned before, this study focuses on acquiring a simple numerical model to compute backwater with high accuracy, which can be implemented on multiple opening bridges and skewed crossings. In order to develop the mathematical method, the results of HEC-RAS software and parametric studies are used. The developed method was compared with the energy method results from HEC-RAS and was validated with the experimental data for its accuracy.

4.1. Parametric Studies on Skewed Crossings

A series of parametric studies were conducted by Atabay et al. indicating the influence of several factors on backwater depth. Such factors included Froude number, area of the main channel, area of floodplain, floodplain width, main channel width, and bridge opening width. According to Atabay et al., the bridge opening width (b) has a negative correlation with backwater depth, as an increase in b results in a decrease in backwater. Moreover, positive relationships between backwater and roughness coefficients as well as discharge values were found; it was found that the main channel roughness coefficients and discharge values have a more significant impact on backwater [27]. Likewise, similar impacts of flow rate and roughness coefficients are anticipated for this study.

In the current study, the impacts of different factors on backwater for skewed bridges are investigated by running different scenarios on HEC-RAS. According to Bradley, for skewed angles up to 20°, the flow pattern shows no objection; however, the flow efficiency decreases as the skew angle increases above 20°. It is worth mentioning here that the implementation of projected length on HEC-RAS is not adequate for skew angles greater than 30° [1, 5]. Therefore, the parametric studies are done on a DECK bridge with a 398 mm wide opening only and skewed angles below 30° with a total of three scenarios. In the first scenario, the impact of main channel roughness coefficient on backwater are investigated by maintaining the floodplain roughness coefficient at a value of 0.050 and discharge value at 30 l/s. The main channel roughness coefficients vary from 0.030 to 0.050 at an increment of 0.005 with skew angles of 0º, 5º, 10º, 15º, 20º, 25º, and 30º. Figure 4.1 represents the variation of backwater depth with the variable n_{mc} for each corresponding skew angle. According

to Figure 4.1, the main channel roughness has a positive correlation with backwater depth; with an increase in main channel roughness, the backwater depth increases.

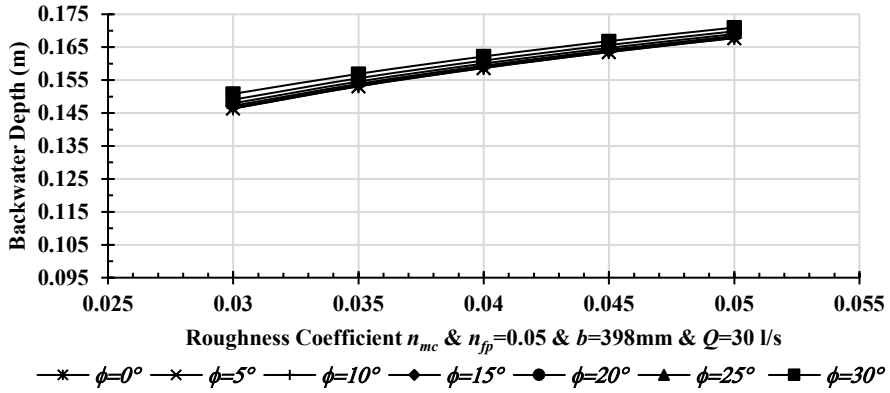

Figure 4.1: Backwater variation with respect to n_{mc}.

In the second scenario, the effect of floodplain roughness on backwater depth is explored by maintaining the discharge value at 30 l/s and the main channel roughness coefficient at 0.03. The floodplain roughness coefficient is then increased from 0.05 to 0.07 at increments of 0.005. Figure 4.2 represents the backwater variation with respect to floodplain roughness coefficient for the corresponding discharge value. It can be noted that the floodplain roughness coefficient affects the backwater value positively, as an increase in the floodplain roughness results an increase in the backwater depth. However, the floodplain roughness coefficient is less effective in comparison with main channel roughness coefficient since it has a smaller positive slope.

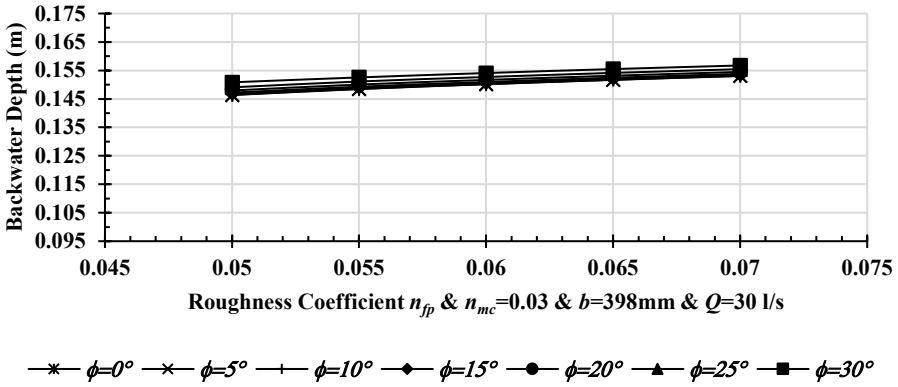

Figure 4.2: Backwater variation with respect to n_{fp}.

In the last scenario, the impact of discharge value on backwater depth is studied by maintaining the floodplain and main channel roughness coefficients at 0.05 and 0.03 respectively. Figure 4.3 emphasizes the relationship between discharge and backwater values for each skew angle. It can be concluded that an increase in the discharge value leads to an increase in the backwater depth. In comparison, the discharge value is found to have a more significant impact on backwater compared to the main channel roughness coefficient as the slope of the graph is steeper.

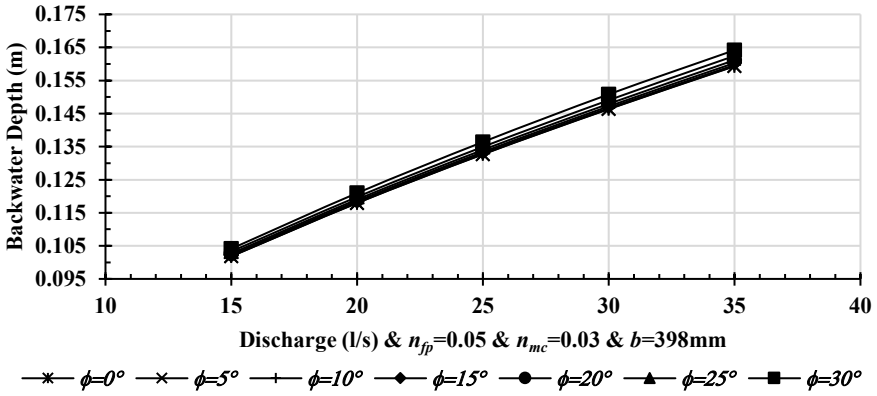

Figure 4.3: Backwater depths in relation to discharge values.

In conclusion, all the scenarios show the same results as anticipated. Although all the scenarios show a positive correlation between the skew angle and backwater depth, the impact of skew angle is not as significant as the other three parameters as all the lines are close to each other.

4.2. Developing the Mathematical Method

4.2.1. Developing the mathematical method for normal bridges. In addition to the current parametric study, Froude number (F) and bridge opening ratio (M') are found to impact backwater significantly in studies conducted by Izzard, Biery and Delleur, Seckin, Seckin et al., and Atabay et al. [14, 15, 19, 21, 27]. Therefore, this study firstly considers these two parameters in the ratio form previously implemented by the other scholars, which is shown in a general format by Eq. 19.

$$\frac{Y_1}{Y_n} = \alpha + \left[\beta \left(\frac{F}{M\prime}\right)^{\gamma}\right] \tag{19}$$

Based on the parametric studies conducted, different scenarios and regression analysis, the above general format is transformed further using main channel discharge (Q_{mc}), total discharge in the channel (Q_{tot}), main channel width (b_{mc}), and total channel width (b_{tot}). Hence, β is taken into consideration as $\frac{Q_{mc}\, b_{mc}}{Q_{tot}\, b_{tot}}$ and γ as $\frac{Q_{tot}}{Q_{mc}}$. In addition, the calculation of the Froude number for compound channel requires more parameter estimations; hence, the Froude number used in this equation is simplified to the Froude number of the main channel. Then, the backwater ratio and $\beta\left(\frac{F_{mc}}{M'}\right)^{\gamma}$ are plotted for normal bridge crossings. Figure 4.4 represents the regression analysis for the best fit line for normal bridges, which suggests a quadratic equation. However, the suggested quadratic equation from the regression analysis does not contain a high level of data precision, and it indicates a necessity of two models to fit the regression analysis. In addition, this formula cannot be applied to skewed crossings as it does not contain a general format. Thus, in order to achieve a single mathematical formula that is applicable to all types of crossings including skewed ones, the trial is discarded.

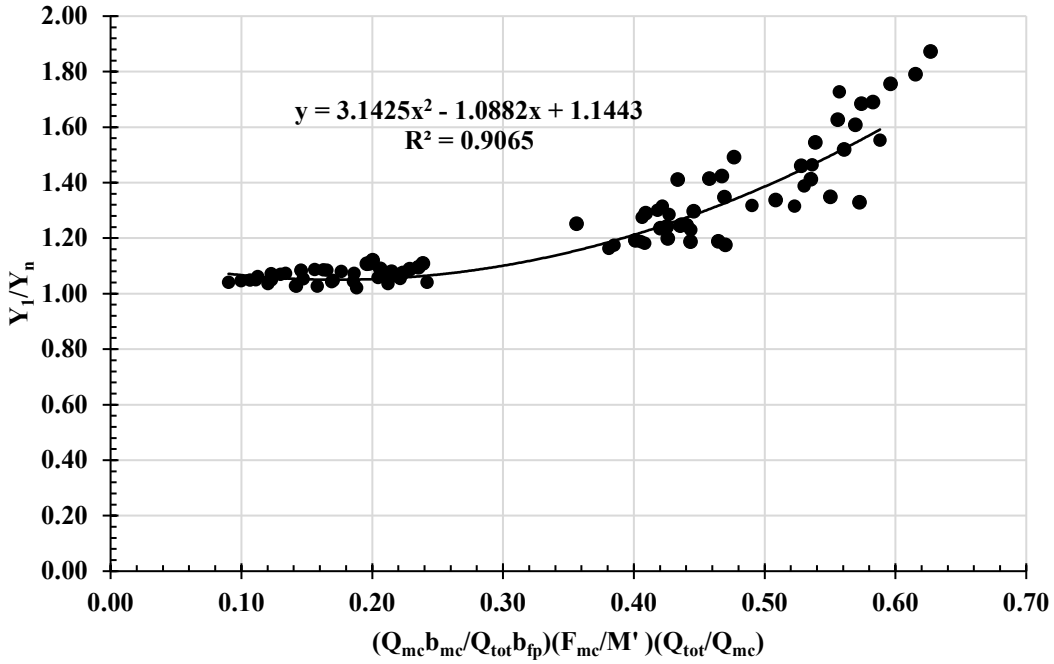

Figure 4.4: Regression analysis of normal bridges for the first trial.

According to the analysis conducted in the study by Atabay et al., α is found to be the most effective parameter in Eq. 19 [27]. Therefore, series of trials are done in

order to adjust the equation for all types of crossings. One of the trials is done by guessing the α value based on trial and error for each bridge shape; however, the values of α that result with errors less than 10.0% vary from 0.78 to 0.94, which is not efficient and practical for the objective of this study (results are presented in Appendix A). Moreover, besides Froude number and opening ratio, blockage ratio (*J*) is found to be another important factor impacting backwater in the literature [21]. Hence, it is implemented as the value for α in another trial. The results for this trial contain a high percentage error ranging from 0.2% to 43.2% for normal bridge crossings (refer to Appendix B).

Furthermore, as the three most effective factors of backwater are found to be Froude number, opening ratio, and blockage ratio a combination of all three in the form of $\left(\frac{F_{mc}}{M\prime}\right)^{J}$ is used to plot with backwater ratio for normal crossings. Figure 4.5 indicates a parabolic relationship between backwater ratio and $\left(\frac{F_{mc}}{M\prime}\right)^{J}$. As the results for the new quadratic equation bring about an absolute average error of 4.4% (refer to Appendix C for detailed results); the regression analysis is applied for skewed bridges to indicate if it results in the same relationship.

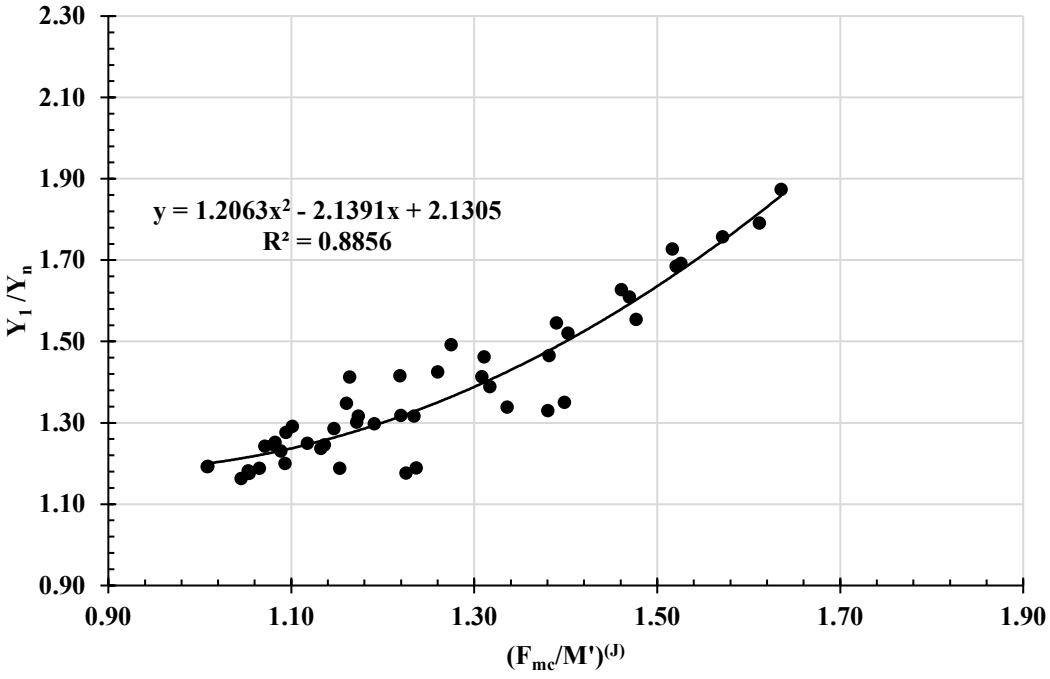

Figure 4.5: Regression analysis for normal bridge crossing using blockage ratio.

4.2.2. Developing the mathematical method for skewed bridges. A skewed crossing usually contains a smaller effective width compared to the normal crossings. It should also be noted that the geometry of arch bridges while being skewed becomes more complex than the skewed DECK bridges [1, 36]. Therefore, the opening ratio and blockage ratio have to be adjusted for the effective area normal to the flow in skewed bridges. In order to adjust the opening ratio, the bridge opening width (b) is considered to be $b' = b \times cos(\phi)$ and for computing A'_{n2}. Likewise, the projected bridge area is computed by multiplying the horizontal dimensions of the bridge by $cos(\phi)$. Moreover, the adjusted ratios are represented by Eq.20 and Eq. 21.

$$M' = \frac{A'_{n2}}{A_{n1}} \tag{20}$$

Where:

M' = the modified opening ratio

A'_{n2} = the normal depth cross-sectional area for the projected bridge opening

A_{n1} = the normal depth cross-sectional area for the channel

$$J = \frac{A'_{nb}}{A_{n1}} \tag{21}$$

Where:

J = the downstream blockage ratio

A'_{nb} = the normal depth cross-sectional area for the projected bridge

A_{n1} = the normal depth cross-sectional area for the channel

Furthermore, since the implementation of projected length on HEC-RAS is not adequate for skew angles greater than 30°, the regression analysis is only done for normal bridge crossing and skewed crossings with ϕ=30°. Figure 4.6 represents the relationship between backwater ratio and $\left(\frac{F_{mc}}{M'}\right)^J$. Similar to the normal crossing regression analysis graph, Figure 4.6 provides a quadratic equation for calculating backwater ratio using $\left(\frac{F_{mc}}{M'}\right)^J$ with the coefficient of determination of 0.90 (refer to Appendix D for detailed results). Thus, the equation can be generalized to be applicable to all types of crossings and bridge shapes.

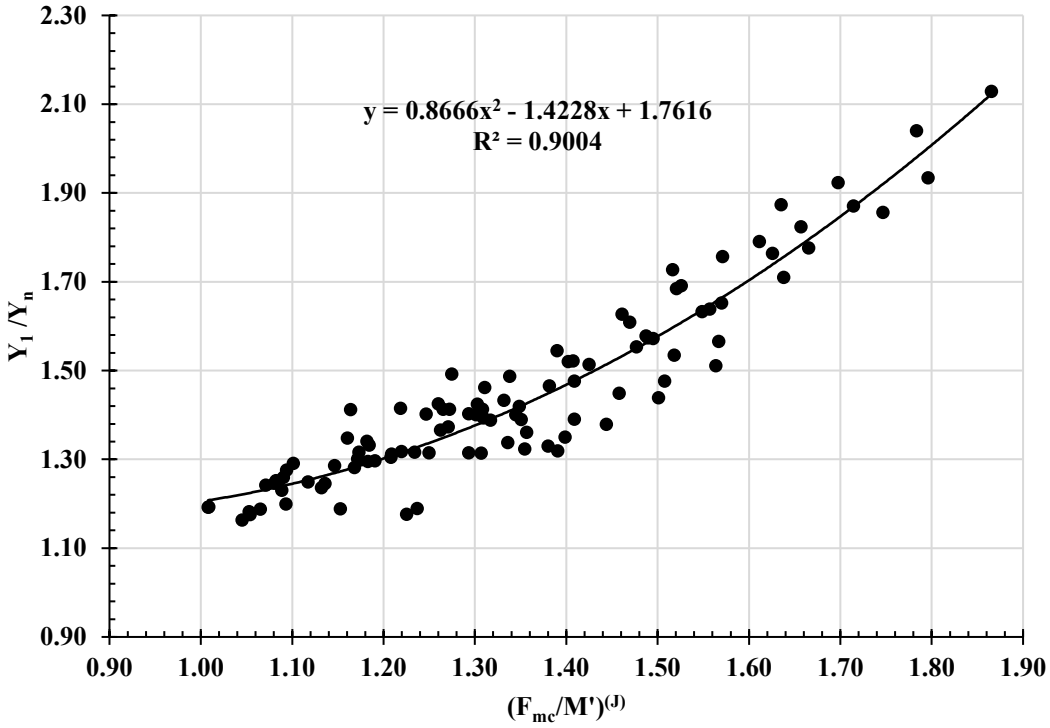

Figure 4.6: Regression analysis for normal and skewed bridge crossings.

After implementing several trials for generalizing the quadratic equation, Eq. 22 is achieved. It should be noted that for skewed crossings, the opening ratio and blockage ratio are used according to Eq. 20 and Eq. 21. A factor of 1.03 is also added to the equation to allow for more accuracy.

$$\frac{Y_1}{Y_n} = 1.03 \times \left[\frac{b_{mc}}{b_{tot}}\left[\left(\frac{F_{mc}}{M'}\right)^J\right]^2 + \frac{b_{mc}}{b_{tot}} \times \frac{Q_{tot}}{Q_{mc}} \times \left(\frac{F_{mc}}{M'}\right)^J + \frac{Q_{tot}}{Q_{mc}}\right] \quad (22)$$

Where:

F_{mc} = the Froude number of the main channel

M' = the modified opening ratio

J = the downstream blockage ratio

Q_{mc} = the main channel discharge

Q_{tot} = the total discharge

b_{mc} = the main channel width

b_{tot} = the total channel width

Chapter 5. Results and Discussion

In this chapter, the application of the proposed method is represented in addition to its comparison with energy method. Also, the performance of the proposed method is evaluated by experimental results.

5.1. Application of the Proposed Method

The normal water depth is computed using the compound channel cross-section without any constrictions using Manning's equation. The discharge values measured in the experimental data, as well as the roughness coefficients, are used to compute the main channel Froude number, the main channel discharge, blockage ratio, and opening ratio. Moreover, literature has shown that the most accurate conventional method of computing backwater is the energy method [2, 4, 27]. Thus, the results of the proposed method are compared with the energy method considering two scenarios. In the first scenario, due to the inadequacy of HEC-RAS for skew angles above 30°, the proposed method is applied for skew angles ranging from 0° to 30°. For these analyses, Case A properties (n_{mc}=0.009 and n_{fp}=0.010) are taken into consideration in order to observe the proposed method performance under different skew angles for all types of bridges. In the second scenario, the proposed method is further evaluated by considering different roughness cases using the three test cases from the experimental data for normal and skewed crossings at 30°.

Furthermore, Table 5.1 represents the results for the skewed AMOSC bridges for skew angles below 30° with the correspondent differences for each result from the energy method only for brevity (for detailed results refer to Appendix E). Accordingly, the proposed method is found to underestimate the backwater compared to the energy method, with percentage differences decreasing as the discharge value increases. Also, it can be noted that with an increase in the skew angle, the percentage differences increase. Additionally, the average percentage difference for all skew angles is found to be 7.7% with the highest percentage of 15.5% and the lowest percentage difference of 4.5% for all the bridges. The overall root-mean-square error (RMSE) is found to be 0.007. As the value of RMSE is found to be very close to zero, it can be concluded that the proposed method and energy method are highly correlated.

Table 5.1: Comparison between computed values by energy method and the proposed method for AMOSC bridges with different skew angles.

Type of Bridge	Skew Angle ϕ	Discharge (l/s)	Proposed Method Y (mm)	Energy Method Y (mm)	Errors (%)
AMOSC	**5°**	18.1	82.9	89.7	10.3
		21.0	94.2	100.5	9.0
		24.0	104.7	110.4	7.9
		29.8	123.9	127.8	5.9
		33.1	133.8	137.8	5.8
		37.9	148.4	151.3	4.8
AMOSC	**10°**	18.1	83.7	92.1	11.7
		21.0	95.1	102.9	10.3
		23.9	105.6	112.5	8.8
		29.7	124.8	130.2	6.9
		33.2	134.7	140.2	6.7
		38.3	149.3	154.0	5.8
AMOSC	**15°**	18.1	85.1	95.4	13.3
		21.0	96.5	105.7	11.3
		23.9	107.1	115.4	9.9
		29.7	126.4	133.5	8.1
		33.2	136.3	143.5	7.8
		38.2	150.9	157.7	7.1
AMOSC	**20°**	18.1	87.2	99.3	14.8
		21.0	98.6	109.5	12.5
		24.0	109.3	119.4	11.2
		29.8	128.5	137.7	9.4
		33.1	138.4	148.1	9.3
		37.9	152.9	162.6	8.7
AMOSC	**25°**	18.1	89.8	103.2	15.4
		21.0	101.4	113.6	13.3
		23.9	112.0	124.2	12.4
		29.7	131.2	142.8	10.8
		33.2	141.0	153.4	10.8
		38.2	155.5	168.6	10.5
AMOSC	**30°**	18.1	93.2	108.9	14.5
		21.0	104.8	119.4	12.2
		23.9	115.4	129.9	11.2
		29.7	134.5	150.1	10.4
		33.2	144.1	161.2	10.6
		38.2	158.4	176.9	10.5

Similar to the results for different skew angles, the proposed method results from different roughness cases contribute to mostly underestimated backwater values in comparison with the energy method. However, there is no certain pattern for the percentage differences as it was the case for the first scenario. For the sake of brevity, the results of ASOE bridges for skew angle at 30° are represented by Table 5.2 (refer to Appendix E for detailed results). Furthermore, the proposed method can be considered to have a good correlation with energy method with an absolute average percentage difference of 6.1% and RMSE of 0.052. However, in order to estimate the level of accuracy of the proposed method, it should be compared with the experimental data as HEC-RAS is inadequate for ϕ=45°.

Table 5.2: Comparison between computed values by energy method and the proposed method for skewed ASOE bridge at ϕ=30°.

Type of Bridge	Test Case	Discharge (l/s)	Proposed Method Y (mm)	Energy Method Y (mm)	Errors (%)
ASOE	**A**	18.1	88.5	94.6	6.5
		21.0	99.5	104.8	5.1
		24.0	109.7	115.2	4.8
		29.8	128.0	134.3	4.6
		33.1	137.4	145.1	5.3
		37.9	151.1	160.3	5.8
ASOE	**B**	18.1	87.6	92.8	5.7
		21.0	103.1	103.8	0.6
		23.9	117.9	113.8	3.6
		29.7	148.0	133.5	10.8
		33.2	167.9	145.0	15.8
		38.3	178.7	161.4	10.7
ASOE	**C**	18.1	86.1	93.6	8.0
		21.0	95.4	104.0	8.3
		23.9	109.9	114.4	4.0
		29.7	146.0	132.7	10.1
		33.2	149.8	144.7	3.5
		38.2	172.0	161.2	6.7

5.2. Validation of the Proposed Method

Evaluation of the proposed method accuracy is done by comparing the results with the experimental data for validation purpose. Hence, the proposed equation is

applied for each experimental data for both normal and skewed crossings. Table 5.3 represents the results for the skewed AMOSC bridges at 30° with the correspondent differences for each result from the experimental data only for brevity (for detailed results refer to Appendix F). As anticipated, there is no specific pattern for the percentage differences based on different test cases. Moreover, the average absolute percentage differences are 6.5%, 5.3%, and 3.7% for normal, skewed at 30°, and skewed at 45° bridge crossings respectively. In addition, the range of the absolute percentage differences are 0.4 to 13.7%, 0.0 to 10.8%, and 0.0 to 11.5% for normal, skewed at 30°, and skewed at 45° bridge crossings respectively. Hence, it can be concluded that the percentage differences decrease as the skew angle increases. Moreover, the overall absolute percentage difference is found to be 5.1% with the overall RMSE value of 0.008, which is relatively very close to zero. Therefore, it can be concluded that the proposed formula is accurate and reliable for all three types of bridge crossing.

Table 5.3: Comparison between experimental values and computed by the proposed method at 30°.

Type of Bridge	Test Case	Discharge (l/s)	Proposed Method Y (mm)	Experimental Data Y (mm)	Errors (%)
AMOSC	**A**	18.1	93.2	100.3	7.1
		21.0	104.8	111.6	6.1
		24.0	115.4	121.4	5.0
		29.8	134.5	140.5	4.3
		33.1	144.1	152.0	5.2
		37.9	158.4	175.1	9.5
AMOSC	**B**	18.1	90.2	97.8	7.7
		21.0	106.2	110.0	3.4
		23.9	121.3	120.8	0.4
		29.7	152.1	144.6	5.2
		33.2	172.6	158.4	8.9
		38.3	181.7	181.8	0.1
AMOSC	**C**	18.1	89.4	98.1	8.9
		21.0	98.4	109.8	10.3
		23.9	113.5	119.3	4.9
		29.7	151.6	139.8	8.4
		33.2	154.4	153.2	0.8
		38.2	177.2	177.3	0.0

In addition to the proposed method, the energy method is also compared with experimental data so that the overall level of accuracy of the proposed method can be evaluated further (refer to Appendix F). The RMSE of energy method and experimental data is found to be 0.042, which is relatively higher than the RMSE value found for the proposed method.

Figure 5.1 illustrates the comparison of backwater values computed by the proposed formula and energy method versus the measured backwater from the experimental data. Accordingly, the proposed formula mostly underestimates the backwater value for all types of crossings. It also indicates that the proposed method has a good correlation with the experimental data. On the other hand, the energy method is found to mostly overestimates the backwater value. In addition, as the proposed method and energy method results are close to each other, it can be concluded that the proposed method can be considered to have a good correlation with the energy method. Additionally, the proposed method has advantages of being simple and applicability for skewed crossings above 30º. Consequently, the proposed method is acknowledged as a simple empirical method for computing backwater for all types of crossings with a high level of accuracy and correlation with energy method as well as experimental data.

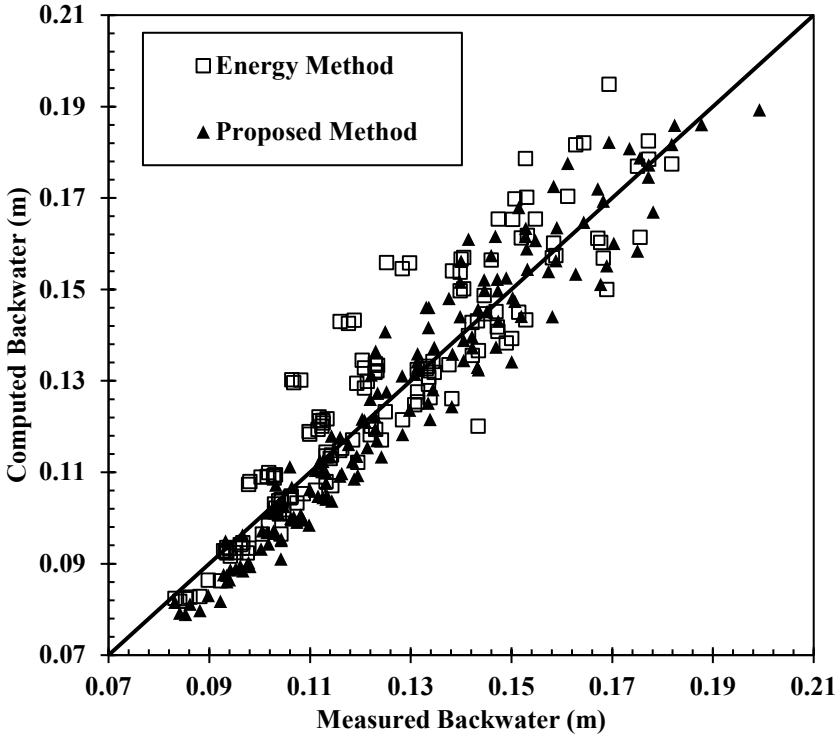

Figure 5.1: Comparison of measured and computed backwater values.

Chapter 6. Conclusion and Future Work

In this thesis, different parameters affecting backwater were evaluated by conducting a series of parametric studies on the main channel roughness coefficient, floodplain roughness coefficient, discharge, and skewness. The parametric studies concluded that main channel roughness coefficient and discharge have the highest impact on backwater value. As a result, the derivation of a simple mathematical method was done based on parametric studies and multiple regression analysis. The method was firstly based on regression analysis on normal and skewed at 30° crossings using blockage ratio, opening ratio, and main channel Froude number. The method was then generalized to be applicable to all types of crossings and bridge shapes considering other factors such as the main channel discharge, the total discharge, the main channel width, and the total channel width.

The proposed method was firstly compared with energy method considering different skew angles based on test case A properties resulting percentage differences of 4.5% to 15.5% with the overall RMSE value of 0.007. Likewise, the proposed method was evaluated under different roughness conditions by comparing the results with the energy method. The comparison resulted in the absolute average percentage difference of 6.1% and RMSE of 0.052. Therefore, it can be concluded that the proposed method and energy method are highly correlated.

In addition, the proposed method was validated by comparing with the experimental data. The results showed an absolute percentage differences of 0.4% to 13.7%, 0.0% to 10.8%, and 0.0% to 11.5% for normal (skewed at 0º), skewed at 30°, and skewed at 45° crossings respectively. In addition, an overall absolute average percentage difference of 5.1% with an overall RMSE value of 0.008 were obtained. Thus, the proposed method is assumed to have high correlations with experimental data. Additionally, as HEC-RAS is inadequate for skew angles above 30° [29], therefore, the energy method results for skewed crossings at 45° contributed to absolute percentage differences ranging from 3.0 to 124.4% with an absolute average percentage difference of 27.1%. Thus, the proposed method has the advantage of being applicable for all skew angles even up to 45°. In addition, the proposed method is beneficial for hydraulic engineers in any stage of designing and analysing bridges.

Conclusively, the results of this study are applicable to both normal and skewed crossings with single and multiple opening bridges. The study considers different shapes of bridge openings under subcritical flow without submerging the bridge low chord or overtopping the roadway. Moreover, the study is objected to a compound channel with different roughness conditions. However, the study is limited to vertical wall abutments and the possible influences of piers, entrance rounding, eccentricity, and scour are not included. Therefore, it is recommended that researchers consider these factors in the future studies.

References

[1] L. Hamill, *Bridge Hydraulics*, London, UK: E & FN SPON, 1999.

[2] S. Atabay, "Accuracy of the ISIS bridge methods for prediction of afflux at high flows," *Water and Environment Journal,* vol. 22, no. 1, pp. 64-73, 2008.

[3] G. W. Brunner and J. H. Hunt, "A comparison of the one-dimensional bridge hydraulic routines from HEC-RAS, HEC-2 and WSPRO," *Research Document no.42*, US Army Corps of Engineers, Davic, CA, 1995.

[4] G. Seckin and S. Atabay, "Experimental backwater analysis around bridge waterways," *Canadian Journal of Civil Engineering,* vol. 32, no. 6, pp. 1015-1029, 2005.

[5] J. N. Bradley, *Hydraulics Of Bridge Waterways: Hydraulic Design*, Series no.1, Washington, DC: US Federal Highway Administration , 1978.

[6] K. S. Erduran, G. Seckin, S. Kocaman and S. Atabay, "3D numerical modeling of flow around skewed bridge crossing," *Engineering Applications of Computational Fluid Mechanics,* vol. 6, no. 3, pp. 475-489, 2012.

[7] G. Seckin, T. Haktanir and D. W. Kinght, "A simple method for estimating flood flow around bridges," *Proceedings of the Institution of Civil Engineers - Water Management,* vol. 160, no. 4, pp. 195-202, 2007.

[8] D. L. Yarnell, "Bridge piers as channel obstructions," *Rep. No. 442,* US Department of Agriculture, Washington, DC, 1934.

[9] J. O. Shearman, "User's manual for WSPRO: A computer model for water surface profile computation," *Rep. No. FHWA-IP-89-027,* US Geological Survey, Federal Highway Administration, Reston, VA, 1990.

[10] V. R. Schneider, J. W. Board, B. E. Colson, F. N. Lee and L. Druffel, "Computation of backwater discharge at width constrictions of heavenly flood plains," *Rep. No. 76-129,* US Geological Survey, Bay St. Louis, 1977.

[11] P. M. Brown, *Afflux at Arch Bridges*, Hydraulic Research Wallingford, Wallingford, 1998.

[12] H. K. Liu, J. N. Bradley and E. J. Plate, "Backwater effects of piers and abutments," *Rep. No. CER57HKIO,* Colorado State University, Boulder, 1957.

[13] H. Tracy and R. Carter, "Backwater effects of open channel constrictions," *Transactions of the American Society of Civil Engineers,* vol. 120, pp. 993-1006, 1955.

[14] C. F. Izzard, "Discussions of "Backwater effects of open-channel constrictions" by H.J. Tracy and R.W. Carter," *Transactions of the Americcan Society of Civil Engineers,* vol. 120, pp. 1008-1013, 1955.

[15] P. Biery and J. Delleur, "Hydraulics of single span arch bridge constrictions," *ASCE Journal of Hydraulic Division,* vol. 88, no. 2, pp. 75-108, 1962.

[16] K. J. Kaatz and W. P. James , "Analysis of alternatives for computing backwater at bridges," *ASCE Journal of Hydraulic Engineering,* vol. 123, no. 9, pp. 784-792, 1997.

[17] B. Biglari and T. W. Sturm, "Numerical modeling of flow around bridge abutments in compound channel," *ASCE Journal of Hydraulic Engineering,* vol. 124, no. 2, pp. 156-164, 1998.

[18] S. Atabay and D. W. Knight, "Bridge afflux experiments in compound channels. Report supplied to JBA Consulting," School of Civil Engineering, University of Birmingham, Birmingham, UK, 2002.

[19] G. Seckin, "A simple formula for estimating backwater at bridge constrictions," *Canadian Journal of Civil Engineering,* vol. 31, no. 4, pp. 561-568, 2004.

[20] G. Seckin, "The effect of skewness on bridge backwater prediction," *Canadian Journal of Civil Engineering,* vol. 34, no. 10, pp. 1371-1374, 2007.

[21] G. Seckin, D. W. Knight, S. Atabay and N. Seckin, "Improving bridge afflux prediction for overbank flows," *Proceedings of the Institution of Civil Engineers,* vol. 161, no. 5, pp. 253-262, 2008.

[22] S. Atabay, J. A. Abdalla, K. Erduran, M. Mortula and G. Seckin, "Prediction of backwater level of bridge constriction using ANN," *Water Management ICE,* vol. 166, no. 10, pp. 556-570, 2012.

[23] G. Seckin, M. S. Akoz, M. Cobaner and T. Haktanir, "Application of ANN techniques for estimating backwater through bridge constrictions in Mississippi river basin," *Advances in Engineering Software,* vol. 40, no. 10, pp. 1039-1046, 2009.

[24] M. Mamak, G. Seckin, M. Cobaner and O. Kisi, "Bridge afflux analysis through arched bridge constrictions using artificial intelligence methods," *Civil Engineering and Environmental Systems,* vol. 26, no. 3, pp. 279-293, 2009.

[25] E. Pinar, G. Seckin, B. Sahin, H. Akilli, M. Cobaner, S. Atabay, C. Canpolat and S. Kocaman, "ANN approaches for prediction of bridge backwater using both field and experimental data," *International Journal of River Basin Management,* vol. 9, no. 1, pp. 53-62, 2011.

[26] S. Atabay, "Stage-discharge, resistance, and sediment transport relationship for flow in straight compound channels," Ph.D thesis, The University of Birmingham, Birmingham, Uk, 2001.

[27] S. Atabay, K. Haji Amou Assar, M. Hashemi and M. Dib, "Prediction of the backwater level due to bridge constriction in waterways," *Water and Envrionment Journal,* vol. 23, no. 1, pp. 94-103, 2018.

[28] K. S. Erduran, G. Seckin, S. Kocaman and S. Atabay, "3D numberical modelling of flow around skewed bridge crossing," *Engineering Applications of Computational Fluids Mechanics,* vol. 6, no. 3, pp. 475-489, 2012.

[29] G. Brunner, HEC-RAS, River analysis system hydraulic reference manual, 4.1, Ed., Davis, CA: US Army Crops of Engineers, 2010.

[30] R. Lamb, P. Mantz, S. Atabay and J. Benn, "Recent advances in modelling flood water level at bridges and culverts," J *Proc. 41st Defra Flood and Coastal Management Conference,* York, UK, 2006.

[31] C. E. Kindsvater and R. W. Carter, "Tranquil flow through open channel constrictions," *Transactions of the American Society of Civil Engineers,* vol. 120, pp. 955-992, 1955.

[32] C. M. Kindsvater, R. W. Carter and H. J. Tracy, "computation of peak discharge at contractions," *Geological Survey Circular 284,* US Geological Survery, Washington, DC, 1953.

[33] O. A. Akan, *Open Channel Hydraulics*, Burlington, MA: Butterworth-Heinemann, 2006.

[34] J. H. Hunt and G. W. Brunner, "Flow Transitions in Bridge Backwater Analysis," *Research Document No. 42,* US Army Corps of Engineers, Davis, California, 1995.

[35] J. H. Hunt, G. W. Brunner and B. E. Larock, "Flow transitions in bridge backwater analysis," *ASCE Journal of Hydraulic Engineering,* vol. 125, no. 9, pp. 981-983, 1999.

[36] S. T. Hussain and G. M. Rao, "Hydraulics of river flow under arch bridges," *Irrigation and Power,* vol. October, pp. 441-454, 1966.

Appendix A

Results of variation of α for each type of bridge shapes for normal crossing

Table A. 1: Results of trial with different α values.

Type of Bridge	Test Case	Discharge (l/s)	Trial Result Y (mm)	Measured Exp. Data Y (mm)	Errors (%)
AMOSC	**A**	21.0	103.3	101.8	1.5
		24.0	108.5	113.2	4.2
		27.0	113.9	124.2	8.3
		30.0	118.9	133.9	11.2
		34.4	127.8	150.1	14.8
AMOSC	**B**	18.0	96.3	89.8	7.2
		21.0	110.0	100.6	9.3
		24.1	121.9	111.1	9.7
		30.0	144.6	131.4	10.0
		34.3	147.1	149.0	1.3
AMOSC	**C**	18.1	95.7	92.3	3.7
		21.0	98.8	104.3	5.3
		23.9	111.3	114.4	2.7
		29.7	145.5	130.8	11.2
		33.2	140.7	142.2	1.1
		38.2	157.7	168.9	6.7
ASOE	**A**	21.0	95.9	97.9	2.0
		24.0	100.9	108.7	7.2
		27.0	106.2	119.5	11.1
		30.0	111.3	128.4	13.3
		34.4	120.7	143.5	15.8
ASOE	**B**	18.0	89.4	86.2	3.6
		21.0	103.1	96.6	6.8
		24.1	115.9	106.0	9.3
		30.0	141.8	125.0	13.5
		34.3	157.0	141.5	10.9
ASOE	**C**	18.1	88.6	85.3	3.9
		21.0	91.6	95.3	3.9
		23.9	104.4	104.8	0.4
		29.7	141.7	123.1	15.2
		33.2	137.3	133.6	2.8
		38.2	157.5	152.9	3.0
DECK	**A**	18.1	92.2	88.2	4.6
		21.0	97.3	97.6	0.3
		24.0	102.0	107.4	5.1
		26.9	113.6	118.5	4.1
		34.3	115.1	138.2	16.7
DECK	**B**	18.1	91.0	83.2	9.3
		21.0	103.2	93.3	10.6
		23.9	114.1	103.2	10.5
		29.7	134.5	122.2	10.1
		33.2	149.3	133.6	11.8
DECK	**C**	18.1	90.0	84.2	6.9
		21.0	92.7	94.2	1.6
		23.9	104.3	103.9	0.3
		29.7	135.4	122.0	11.0
		33.2	130.5	131.4	0.7
		38.2	144.8	147.4	1.8

Appendix B

Results of implementing J for α for normal crossing

Table B.1: Results of replacing blockage ratio with α.

Type of Bridge	Test Case	Discharge (l/s)	Trial Result Y (mm)	Measured Exp. Data Y (mm)	Errors (%)
AMOSC	**A**	21.0	128.8	101.8	26.6
		24.0	131.4	113.2	16.1
		27.0	134.6	124.2	8.4
		30.0	137.8	133.9	3.0
		34.4	144.1	150.1	4.0
AMOSC	**B**	18.0	120.4	89.8	34.0
		21.0	127.3	100.6	26.6
		24.1	134.3	111.1	20.8
		30.0	148.8	131.4	13.3
		34.3	148.5	149.0	0.4
AMOSC	**C**	18.1	122.1	92.3	32.3
		21.0	121.7	104.3	16.7
		23.9	128.8	114.4	12.6
		29.7	153.0	130.8	17.0
		33.2	147.7	142.2	3.8
		38.2	159.9	168.9	5.4
ASOE	**A**	21.0	126.6	97.9	29.3
		24.0	129.2	108.7	18.9
		27.0	132.6	119.5	11.0
		30.0	136.1	128.4	6.0
		34.4	143.2	143.5	0.2
ASOE	**B**	18.0	118.7	86.2	37.6
		21.0	126.5	96.6	31.0
		24.1	135.0	106.0	27.3
		30.0	154.1	125.0	23.3
		34.3	165.4	141.5	16.9
ASOE	**C**	18.1	120.1	85.3	40.8
		21.0	120.0	95.3	25.9
		23.9	127.9	104.8	22.0
		29.7	156.7	123.1	27.3
		33.2	151.8	133.6	13.6
		38.2	168.0	152.9	9.9
DECK	**A**	18.1	92.2	88.2	4.6
		21.0	97.3	97.6	0.3
		24.0	102.0	107.4	5.1
		26.9	113.6	118.5	4.1
		34.3	115.1	138.2	16.7
DECK	**B**	18.1	91.0	83.2	9.3
		21.0	103.2	93.3	10.6
		23.9	114.1	103.2	10.5
		29.7	134.5	122.2	10.1
		33.2	149.3	133.6	11.8
DECK	**C**	18.1	90.0	84.2	6.9
		21.0	92.7	94.2	1.6
		23.9	104.3	103.9	0.3
		29.7	135.4	122.0	11.0
		33.2	130.5	131.4	0.7
		38.2	144.8	147.4	1.8

Appendix C

Results of regression analysis equation for normal crossings

Table C.1: Results of regression analysis equation for normal crossings.

Type of Bridge	Test Case	Discharge (l/s)	Trial Result Y (mm)	Measured Exp. Data Y (mm)	Errors (%)
AMOSC	**A**	21.0	103.3	101.8	1.4
		24.0	114.1	113.2	0.8
		27.0	125.0	124.2	0.7
		30.0	134.9	133.9	0.8
		34.4	151.3	150.1	0.8
AMOSC	**B**	18.0	86.1	89.8	4.1
		21.0	99.3	100.6	1.2
		24.1	111.1	111.1	0.0
		30.0	133.0	131.4	1.2
		34.3	139.1	149.0	6.7
AMOSC	**C**	18.1	86.2	92.3	6.6
		21.0	91.5	104.3	12.3
		23.9	104.4	114.4	8.7
		29.7	137.4	130.8	5.0
		33.2	134.7	142.2	5.3
		38.2	151.4	168.9	10.4
ASOE	**A**	21.0	96.1	97.9	1.8
		24.0	106.7	108.7	1.8
		27.0	117.9	119.5	1.3
		30.0	128.7	128.4	0.3
		34.4	147.8	143.5	3.0
ASOE	**B**	18.0	84.5	86.2	2.0
		21.0	98.3	96.6	1.8
		24.1	112.1	106.0	5.7
		30.0	140.0	125.0	12.0
		34.3	156.7	141.5	10.7
ASOE	**C**	18.1	83.1	85.3	2.5
		21.0	88.8	95.3	6.8
		23.9	102.7	104.8	2.0
		29.7	145.2	123.1	18.0
		33.2	142.2	133.6	6.5
		38.2	166.4	152.9	8.8
DECK	**A**	18.1	86.9	88.2	1.4
		21.0	96.6	97.6	1.0
		24.0	106.0	107.4	1.4
		26.9	123.5	118.5	4.3
		34.3	132.4	138.2	4.1
DECK	**B**	18.1	84.8	83.2	1.9
		21.0	96.9	93.3	3.9
		23.9	107.8	103.2	4.5
		29.7	128.7	122.2	5.3
		33.2	142.9	133.6	7.0
DECK	**C**	18.1	83.4	84.2	1.0
		21.0	88.5	94.2	6.0
		23.9	100.4	103.9	3.4
		29.7	129.4	122.0	6.1
		33.2	127.8	131.4	2.7
		38.2	142.1	147.4	3.6

Appendix D

Results of regression analysis equation for normal and skewed crossings

Table D.1: Results of regression analysis equation for normal crossings.

Type of Bridge	Test Case	Discharge (l/s)	Trial Result Y (mm)	Measured Exp. Data Y (mm)	Errors (%)
AMOSC	**A**	21.0	101.0	101.8	0.8
		24.0	110.6	113.2	2.3
		27.0	120.0	124.2	3.4
		30.0	128.6	133.9	4.0
		34.4	142.6	150.1	5.0
AMOSC	**B**	18.0	86.7	89.8	3.5
		21.0	99.9	100.6	0.7
		24.1	111.7	111.1	0.5
		30.0	133.7	131.4	1.8
		34.3	140.0	149.0	6.0
AMOSC	**C**	18.1	86.5	92.3	6.2
		21.0	91.8	104.3	12.0
		23.9	104.4	114.4	8.7
		29.7	136.1	130.8	4.0
		33.2	134.1	142.2	5.7
		38.2	150.6	168.9	10.9
ASOE	**A**	21.0	95.2	97.9	2.8
		24.0	104.6	108.7	3.8
		27.0	114.3	119.5	4.3
		30.0	123.7	128.4	3.7
		34.4	139.9	143.5	2.5
ASOE	**B**	18.0	85.0	86.2	1.4
		21.0	99.0	96.6	2.5
		24.1	112.5	106.0	6.1
		30.0	139.8	125.0	11.9
		34.3	156.4	141.5	10.5
ASOE	**C**	18.1	83.7	85.3	1.9
		21.0	89.4	95.3	6.2
		23.9	102.9	104.8	1.8
		29.7	142.5	123.1	15.8
		33.2	140.4	133.6	5.1
		38.2	162.8	152.9	6.5
DECK	**A**	18.1	86.8	88.2	1.6
		21.0	95.6	97.6	2.1
		24.0	104.0	107.4	3.2
		26.9	119.5	118.5	0.9
		34.3	127.4	138.2	7.8
DECK	**B**	18.1	85.4	83.2	2.6
		21.0	97.6	93.3	4.6
		23.9	108.6	103.2	5.2
		29.7	129.6	122.2	6.0
		33.2	143.9	133.6	7.7
DECK	**C**	18.1	84.0	84.2	0.3
		21.0	89.1	94.2	5.4
		23.9	100.8	103.9	3.0
		29.7	129.4	122.0	6.1
		33.2	128.2	131.4	2.4
		38.2	142.6	147.4	3.3

Table D.2: Results of regression analysis equation for skewed crossings at 30º.

Type of Bridge	Test Case	Discharge (l/s)	Proposed Method Y (mm)	Measured Exp. Data Y (mm)	Errors (%)
AMOSC	**A**	18.1	102.3	100.3	1.9
		21.0	114.3	111.6	2.5
		24.0	126.0	121.4	3.7
		29.8	148.0	140.5	5.4
		33.1	159.6	152.0	5.0
		37.9	177.8	175.1	1.6
AMOSC	**B**	18.1	94.3	97.8	3.5
		21.0	110.4	110.0	0.3
		23.9	125.5	120.8	3.9
		29.7	156.3	144.6	8.1
		33.2	178.4	158.4	12.7
		38.3	171.8	181.8	5.5
AMOSC	**C**	18.1	95.1	98.1	3.1
		21.0	101.1	109.8	7.9
		23.9	117.3	119.3	1.7
		29.7	162.9	139.8	16.5
		33.2	159.5	153.2	4.1
		38.2	184.3	177.3	3.9
ASOE	**A**	18.1	96.6	96.7	0.1
		21.0	107.5	106.3	1.2
		24.0	118.1	116.3	1.6
		29.8	138.4	134.4	3.0
		33.1	149.1	147.0	1.4
		37.9	165.9	167.8	1.1
ASOE	**B**	18.1	91.3	92.9	1.7
		21.0	106.6	103.8	2.7
		23.9	121.1	114.3	5.9
		29.7	150.7	137.6	9.5
		33.2	171.9	151.5	13.5
		38.3	166.5	175.5	5.2
ASOE	**C**	18.1	91.2	93.5	2.5
		21.0	97.1	104.3	6.9
		23.9	112.4	113.2	0.7
		29.7	155.3	133.1	16.6
		33.2	152.5	144.6	5.5
		38.2	176.1	167.2	5.3
DECK	**A**	18.1	97.8	96.2	1.6
		21.0	108.0	106.2	1.7
		24.0	117.4	115.9	1.2
		29.8	134.1	133.5	0.4
		33.1	142.3	143.3	0.7
		37.9	154.4	158.2	2.4
DECK	**B**	18.1	91.2	93.5	2.5
		21.0	104.2	103.0	1.2
		23.9	115.5	114.0	1.3
		29.7	136.6	134.7	1.4
		33.2	151.1	147.2	2.7
		38.3	149.4	168.3	11.2
DECK	**C**	18.1	91.6	94.0	2.5
		21.0	96.8	104.3	7.2
		23.9	109.4	113.2	3.3
		29.7	139.6	131.3	6.3
		33.2	137.5	142.2	3.3
		38.2	152.2	158.9	4.2

Appendix E

Results of proposed method and energy method for skewed crossings

Table E.1: The results of the proposed method and energy method for skewed ASOE bridges.

Type of Bridge	Skew Angle ϕ	Discharge (l/s)	Proposed Method Y (mm)	Energy Method Y (mm)	Errors (%)
ASOE	**5°**	18.1	79.2	84.7	9.2
		21.0	89.8	94.2	7.4
		24.0	99.8	103.2	6.1
		29.8	118.1	120.5	4.9
		33.1	127.5	130.5	5.1
		37.9	141.4	143.9	4.6
ASOE	**10°**	18.1	79.9	85.2	9.0
		21.0	90.6	94.7	7.1
		23.9	100.6	104.0	6.1
		29.7	118.9	121.5	5.0
		33.2	128.4	130.9	4.8
		38.3	142.3	144.6	4.5
ASOE	**15°**	18.1	81.1	86.2	8.6
		21.0	92.0	96.4	7.4
		23.9	102.0	105.7	6.3
		29.7	120.4	123.5	5.3
		33.2	129.8	133.2	5.4
		38.2	143.7	146.8	4.9
ASOE	**20°**	18.1	83.0	88.1	8.5
		21.0	93.9	98.4	7.4
		24.0	104.0	107.9	6.4
		29.8	122.4	125.8	5.6
		33.1	131.8	135.7	5.6
		37.9	145.7	149.9	5.6
ASOE	**25°**	18.1	85.4	90.6	8.5
		21.0	96.4	100.8	7.2
		23.9	106.5	110.9	6.7
		29.7	125.0	129.2	6.1
		33.2	134.4	139.9	6.8
		38.2	148.2	154.3	6.7
ASOE	**30°**	18.1	88.5	94.6	6.5
		21.0	99.5	104.8	5.1
		23.9	109.7	115.2	4.8
		29.7	128.0	134.3	4.6
		33.2	137.4	145.1	5.3
		38.2	151.1	160.3	5.8

Table E.2: The results of the proposed method and energy method for skewed DECK bridges.

Type of Bridge	Skew Angle ϕ	Discharge (l/s)	Proposed Method Y (mm)	Energy Method Y (mm)	Errors (%)
DECK	**5°**	18.1	79.9	83.7	7.3
		21.0	90.1	93.3	6.2
		24.0	99.3	102.8	6.2
		29.8	115.5	119.6	6.3
		33.1	123.5	128.8	6.9
		37.9	134.8	141.7	7.6
DECK	**10°**	18.1	80.7	84.4	7.2
		21.0	90.9	94.3	6.4
		23.9	100.1	103.5	6.1
		29.7	116.3	120.8	6.6
		33.2	124.3	129.7	6.9
		38.3	135.6	142.5	7.6
DECK	**15°**	18.1	82.0	85.9	7.4
		21.0	92.3	95.6	6.3
		23.9	101.5	105.1	6.2
		29.7	117.7	122.3	6.6
		33.2	125.7	131.6	7.3
		38.2	137.0	144.4	7.9
DECK	**20°**	18.1	83.8	87.6	7.1
		21.0	94.2	97.6	6.3
		24.0	103.5	107.3	6.4
		29.8	119.6	124.9	7.1
		33.1	127.6	134.2	7.7
		37.9	138.9	147.3	8.5
DECK	**25°**	18.1	86.3	90.4	7.3
		21.0	96.7	100.5	6.5
		23.9	106.0	110.3	6.7
		29.7	122.1	128.6	7.8
		33.2	130.1	137.7	8.3
		38.2	141.2	151.0	9.2
DECK	**30°**	18.1	89.5	94.2	5.0
		21.0	99.9	104.5	4.5
		23.9	109.1	114.7	4.9
		29.7	125.1	133.2	6.0
		33.2	133.0	143.1	7.1
		38.2	144.0	156.9	8.2

Table E.3: The results of the proposed method and energy method for normal crossings.

Type of Bridge	Test Case	Discharge (l/s)	Proposed Method Y (mm)	Energy Method Y (mm)	Errors (%)
AMOSC	**A**	21.0	94.3	98.4	4.2
		24.0	104.1	108.0	3.6
		27.0	113.4	117.1	3.2
		30.0	121.6	126.3	3.7
		34.4	134.2	139.3	3.7
AMOSC	**B**	18.0	83.1	86.4	3.9
		21.0	97.2	96.5	0.7
		24.1	110.4	106.1	4.1
		30.0	135.9	125.4	8.4
		34.3	152.5	138.3	10.3
AMOSC	**C**	18.1	81.8	86.3	5.2
		21.0	91.0	96.5	5.7
		23.9	103.7	107.1	3.1
		29.7	131.4	124.8	5.3
		33.2	137.3	135.5	1.3
		38.2	155.2	150.0	3.5
ASOE	**A**	21.0	89.4	93.4	4.3
		24.0	99.5	105.3	5.5
		27.0	109.3	112.2	2.6
		30.0	118.2	121.5	2.7
		34.4	132.4	136.6	3.1
ASOE	**B**	18.0	81.2	82.7	1.9
		21.0	96.2	93.4	3.1
		24.1	111.2	104.4	6.5
		30.0	140.7	123.2	14.2
		34.3	160.9	139.9	15.0
ASOE	**C**	18.1	78.9	82.3	4.1
		21.0	88.9	92.4	3.9
		23.9	102.5	101.8	0.7
		29.7	136.4	119.4	14.3
		33.2	141.6	129.3	9.6
		38.2	163.4	143.4	14.0
DECK	**A**	18.1	79.8	82.8	3.7
		21.0	89.8	92.3	2.8
		24.0	99.1	103.3	4.1
		26.9	112.3	117.1	4.1
		34.3	124.3	126.1	1.4
DECK	**B**	18.1	81.6	82.4	1.0
		21.0	94.9	92.6	2.5
		23.9	107.2	102.2	4.9
		29.7	131.3	120.1	9.4
		33.2	146.0	130.8	11.6
DECK	**C**	18.1	79.2	81.8	3.2
		21.0	88.6	91.7	3.3
		23.9	100.7	100.9	0.1
		29.7	125.9	118.2	6.5
		33.2	133.0	127.6	4.3
		38.2	149.7	140.8	6.3

Table E.4: The results of the proposed method and energy method for skewed crossing at 30º.

Type of Bridge	Test Case	Discharge (l/s)	Proposed Method Y (mm)	Energy Method Y (mm)	Errors (%)
AMOSC	**A**	18.1	93.2	108.9	14.5
		21.0	104.8	119.4	12.2
		24.0	115.4	129.9	11.2
		29.8	134.5	150.1	10.4
		33.1	144.1	161.2	10.6
		37.9	158.4	176.9	10.5
AMOSC	**B**	18.1	90.2	107.3	15.9
		21.0	106.2	118.3	10.2
		23.9	121.3	128.4	5.5
		29.7	152.1	148.6	2.3
		33.2	172.6	160.1	7.8
		38.3	181.7	177.5	2.4
AMOSC	**C**	18.1	89.4	108.0	17.2
		21.0	98.4	118.9	17.2
		23.9	113.5	129.5	12.4
		29.7	151.6	149.7	1.2
		33.2	154.4	161.8	4.6
		38.2	177.2	178.5	0.7
ASOE	**A**	18.1	88.5	94.6	6.5
		21.0	99.5	104.8	5.1
		24.0	109.7	115.2	4.8
		29.8	128.0	134.3	4.6
		33.1	137.4	145.1	5.3
		37.9	151.1	160.3	5.8
ASOE	**B**	18.1	87.6	92.8	5.7
		21.0	103.1	103.8	0.6
		23.9	117.9	113.8	3.6
		29.7	148.0	133.5	10.8
		33.2	167.9	145.0	15.8
		38.3	178.7	161.4	10.7
ASOE	**C**	18.1	86.1	93.6	8.0
		21.0	95.4	104.0	8.3
		23.9	109.9	114.4	4.0
		29.7	146.0	132.7	10.1
		33.2	149.8	144.7	3.5
		38.2	172.0	161.2	6.7
DECK	**A**	18.1	89.5	94.2	5.0
		21.0	99.9	104.5	4.5
		24.0	109.1	114.7	4.9
		29.8	125.1	133.2	6.0
		33.1	133.0	143.1	7.1
		37.9	144.0	156.9	8.2
DECK	**B**	18.1	87.5	92.3	5.2
		21.0	101.1	103.1	1.9
		23.9	113.4	113.0	0.4
		29.7	137.3	131.9	4.1
		33.2	152.2	141.8	7.3
		38.3	169.3	156.8	7.9
DECK	**C**	18.1	86.5	93.3	7.3
		21.0	95.1	103.6	8.2
		23.9	107.6	113.6	5.3
		29.7	134.2	132.5	1.3
		33.2	139.7	142.8	2.2
		38.2	156.3	157.4	0.7

Table E.5: The results of the proposed method and energy method for skewed crossing at 45º.

Type of Bridge	Test Case	Discharge (l/s)	Proposed Method Y (mm)	Energy Method Y (mm)	Errors (%)
AMOSC	**A**	18.1	106.7	130.2	18.1
		21.0	117.7	143.0	17.7
		24.0	127.6	155.8	18.2
		29.8	145.2	325.8	55.4
		33.1	153.9	331.0	53.5
		37.9	166.9	339.2	50.8
AMOSC	**B**	18.1	100.2	129.6	22.7
		21.0	116.1	142.6	18.6
		23.9	131.1	154.6	15.2
		29.7	161.6	178.6	9.5
		33.2	182.2	194.9	6.5
		38.3	189.3	249.7	24.2
AMOSC	**C**	18.1	100.7	130.1	22.6
		21.0	108.6	143.3	24.2
		23.9	123.6	155.8	20.7
		29.7	161.6	329.0	50.9
		33.2	163.5	334.4	51.1
		38.2	185.9	343.2	45.8
ASOE	**A**	18.1	101.3	110.0	7.9
		21.0	112.0	122.1	8.3
		24.0	121.6	134.5	9.6
		29.8	138.8	157.0	11.6
		33.1	147.4	169.8	13.2
		37.9	160.1	334.4	52.1
ASOE	**B**	18.1	96.8	109.1	11.2
		21.0	112.5	121.3	7.2
		23.9	127.3	133.4	4.5
		29.7	157.4	156.4	0.6
		33.2	177.6	170.4	4.2
		38.3	186.1	342.9	45.7
ASOE	**C**	18.1	96.7	109.5	11.7
		21.0	104.9	121.7	13.8
		23.9	119.5	133.7	10.6
		29.7	156.2	156.6	0.3
		33.2	158.9	170.1	6.6
		38.2	180.8	340.2	46.8
DECK	**A**	18.1	102.5	109.4	6.3
		21.0	112.4	121.3	7.4
		24.0	121.0	132.8	8.9
		29.8	135.9	154.1	11.8
		33.1	143.1	165.4	13.5
		37.9	153.3	181.6	15.6
DECK	**B**	18.1	96.7	108.7	11.1
		21.0	110.1	120.1	8.3
		23.9	122.2	131.9	7.4
		29.7	145.7	120.1	21.3
		33.2	160.7	165.4	2.8
		38.3	174.6	182.5	4.3
DECK	**C**	18.1	97.1	109.2	11.0
		21.0	104.5	120.8	13.5
		23.9	116.9	132.2	11.5
		29.7	144.1	153.8	6.3
		33.2	148.1	165.3	10.4
		38.2	164.7	182.0	9.5

Appendix F

Results of energy method and experimental data for all the crossings

Table F.1: The results of the proposed method and experimental data for normal crossing.

Type of Bridge	Test Case	Discharge (l/s)	Proposed Method Y (mm)	Measured Exp. Data Y (mm)	Errors (%)
AMOSC	**A**	21.0	94.3	101.8	7.4
		24.0	104.1	113.2	8.0
		27.0	113.4	124.2	8.7
		30.0	121.6	133.9	9.2
		34.4	134.2	150.1	10.6
AMOSC	**B**	18.0	83.1	89.8	7.5
		21.0	97.2	100.6	3.4
		24.1	110.4	111.1	0.6
		30.0	135.9	131.4	3.4
		34.3	152.5	149.0	2.3
AMOSC	**C**	18.1	81.8	92.3	11.4
		21.0	91.0	104.3	12.7
		23.9	103.7	114.4	9.3
		29.7	131.4	130.8	0.5
		33.2	137.3	142.2	3.5
		38.2	155.2	168.9	8.1
ASOE	**A**	21.0	89.4	97.9	8.7
		24.0	99.5	108.7	8.4
		27.0	109.3	119.5	8.5
		30.0	118.2	128.4	7.9
		34.4	132.4	143.5	7.7
ASOE	**B**	18.0	81.2	86.2	5.9
		21.0	96.2	96.6	0.4
		24.1	111.2	106.0	4.8
		30.0	140.7	125.0	12.6
		34.3	160.9	141.5	13.7
ASOE	**C**	18.1	78.9	85.3	7.5
		21.0	88.9	95.3	6.8
		23.9	102.5	104.8	2.2
		29.7	136.4	123.1	10.9
		33.2	141.6	133.6	6.0
		38.2	163.4	152.9	6.9
DECK	**A**	18.1	79.8	88.2	9.5
		21.0	89.8	97.6	8.0
		24.0	99.1	107.4	7.8
		26.9	112.3	118.5	5.2
		34.3	124.3	138.2	10.0
DECK	**B**	18.1	81.6	83.2	2.0
		21.0	94.9	93.3	1.8
		23.9	107.2	103.2	3.8
		29.7	131.3	122.2	7.5
		33.2	146.0	133.6	9.3
DECK	**C**	18.1	79.2	84.2	5.9
		21.0	88.6	94.2	5.9
		23.9	100.7	103.9	3.1
		29.7	125.9	122.0	3.3
		33.2	133.0	131.4	1.3
		38.2	149.7	147.4	1.6

Table F.2: The results of the proposed method and experimental data for skewed crossing at 30°.

Type of Bridge	Test Case	Discharge (l/s)	Proposed Method Y (mm)	Measured Exp. Data Y (mm)	Errors (%)
AMOSC	**A**	18.1	93.2	100.3	7.1
		21.0	104.8	111.6	6.1
		24.0	115.4	121.4	5.0
		29.8	134.5	140.5	4.3
		33.1	144.1	152.0	5.2
		37.9	158.4	175.1	9.5
AMOSC	**B**	18.1	90.2	97.8	7.7
		21.0	106.2	110.0	3.4
		23.9	121.3	120.8	0.4
		29.7	152.1	144.6	5.2
		33.2	172.6	158.4	8.9
		38.3	181.7	181.8	0.1
AMOSC	**C**	18.1	89.4	98.1	8.9
		21.0	98.4	109.8	10.3
		23.9	113.5	119.3	4.9
		29.7	151.6	139.8	8.4
		33.2	154.4	153.2	0.8
		38.2	177.2	177.3	0.0
ASOE	**A**	18.1	88.5	96.7	8.5
		21.0	99.5	106.3	6.4
		24.0	109.7	116.3	5.7
		29.8	128.0	134.4	4.7
		33.1	137.4	147.0	6.5
		37.9	151.1	167.8	9.9
ASOE	**B**	18.1	87.6	92.9	5.7
		21.0	103.1	103.8	0.6
		23.9	117.9	114.3	3.1
		29.7	148.0	137.6	7.6
		33.2	167.9	151.5	10.8
		38.3	178.7	175.5	1.8
ASOE	**C**	18.1	86.1	93.5	7.9
		21.0	95.4	104.3	8.6
		23.9	109.9	113.2	3.0
		29.7	146.0	133.1	9.7
		33.2	149.8	144.6	3.6
		38.2	172.0	167.2	2.9
DECK	**A**	18.1	89.5	96.2	7.0
		21.0	99.9	106.2	5.9
		24.0	109.1	115.9	5.9
		29.8	125.1	133.5	6.3
		33.1	133.0	143.3	7.2
		37.9	144.0	158.2	8.9
DECK	**B**	18.1	87.5	93.5	6.5
		21.0	101.1	103.0	1.8
		23.9	113.4	114.0	0.5
		29.7	137.3	134.7	1.9
		33.2	152.2	147.2	3.4
		38.3	169.3	168.3	0.6
DECK	**C**	18.1	86.5	94.0	8.0
		21.0	95.1	104.3	8.9
		23.9	107.6	113.2	5.0
		29.7	134.2	131.3	2.2
		33.2	139.7	142.2	1.8
		38.2	156.3	158.9	1.6

Table F.3: The results of the proposed method and experimental data for skewed crossing at 45°.

Type of Bridge	Test Case	Discharge (l/s)	Proposed Method Y (mm)	Measured Exp. Data Y (mm)	Errors (%)
AMOSC	**A**	18.1	106.7	106.4	0.3
		21.0	117.7	116.0	1.4
		24.0	127.6	125.2	1.9
		29.8	145.2	145.2	0.0
		33.1	153.9	157.4	2.2
		37.9	166.9	178.2	6.3
AMOSC	**B**	18.1	100.2	106.8	6.2
		21.0	116.1	117.7	1.4
		23.9	131.1	128.3	2.2
		29.7	161.6	152.8	5.8
		33.2	182.2	169.4	7.6
		38.3	189.3	199.2	5.0
AMOSC	**C**	18.1	100.7	108.2	6.9
		21.0	108.6	118.8	8.6
		23.9	123.6	129.8	4.8
		29.7	161.6	146.8	10.1
		33.2	163.5	159.1	2.8
		38.2	185.9	182.4	1.9
ASOE	**A**	18.1	101.3	101.8	0.5
		21.0	112.0	111.8	0.2
		24.0	121.6	120.4	1.0
		29.8	138.8	140.5	1.2
		33.1	147.4	150.7	2.2
		37.9	160.1	170.4	6.0
ASOE	**B**	18.1	96.8	101.5	4.6
		21.0	112.5	112.0	0.5
		23.9	127.3	123.4	3.2
		29.7	157.4	146.0	7.8
		33.2	177.6	161.2	10.2
		38.3	186.1	187.8	0.9
ASOE	**C**	18.1	96.7	103.2	6.3
		21.0	104.9	113.4	7.5
		23.9	119.5	123.0	2.8
		29.7	156.2	140.0	11.5
		33.2	158.9	153.1	3.8
		38.2	180.8	173.5	4.2
DECK	**A**	18.1	102.5	103.0	0.5
		21.0	112.4	112.6	0.2
		24.0	121.0	120.8	0.2
		29.8	135.9	138.3	1.8
		33.1	143.1	147.4	2.9
		37.9	153.3	162.8	5.8
DECK	**B**	18.1	96.7	102.9	6.0
		21.0	110.1	112.4	2.0
		23.9	122.2	122.9	0.6
		29.7	145.7	143.4	1.6
		33.2	160.7	154.8	3.8
		38.3	174.6	177.2	1.5
DECK	**C**	18.1	97.1	102.8	5.5
		21.0	104.5	112.6	7.2
		23.9	116.9	123.3	5.2
		29.7	144.1	139.8	3.0
		33.2	148.1	150.3	1.4
		38.2	164.7	164.4	0.2

Table F.4: The results of the energy method and experimental data for normal crossing.

Type of Bridge	Test Case	Discharge (l/s)	Energy Method Y (mm)	Measured Exp. Data Y (mm)	Errors (%)
AMOSC	**A**	21.0	101.8	98.4	3.3
		24.0	113.2	108.0	4.6
		27.0	124.2	117.1	5.7
		30.0	133.9	126.3	5.7
		34.4	150.1	139.3	7.2
AMOSC	**B**	18.0	89.8	86.4	3.8
		21.0	100.6	96.5	4.1
		24.1	111.1	106.1	4.5
		30.0	131.4	125.4	4.6
		34.3	149.0	138.3	7.2
AMOSC	**C**	18.1	92.3	86.3	6.5
		21.0	104.3	96.5	7.5
		23.9	114.4	107.1	6.4
		29.7	130.8	124.8	4.6
		33.2	142.2	135.5	4.7
		38.2	168.9	150.0	11.2
ASOE	**A**	21.0	97.9	93.4	4.6
		24.0	108.7	105.3	3.1
		27.0	119.5	112.2	6.1
		30.0	128.4	121.5	5.4
		34.4	143.5	136.6	4.8
ASOE	**B**	18.0	86.2	82.7	4.1
		21.0	96.6	93.4	3.3
		24.1	106.0	104.4	1.5
		30.0	125.0	123.2	1.4
		34.3	141.5	139.9	1.1
ASOE	**C**	18.1	85.3	82.3	3.5
		21.0	95.3	92.4	3.0
		23.9	104.8	101.8	2.9
		29.7	123.1	119.4	3.0
		33.2	133.6	129.3	3.2
		38.2	152.9	143.4	6.2
DECK	**A**	18.1	88.2	82.8	6.0
		21.0	97.6	92.3	5.4
		24.0	107.4	103.3	3.9
		26.9	118.5	117.1	1.2
		34.3	138.2	126.1	8.7
DECK	**B**	18.1	83.2	82.4	1.0
		21.0	93.3	92.6	0.7
		23.9	103.2	102.2	1.0
		29.7	122.2	120.1	1.7
		33.2	133.6	130.8	2.1
DECK	**C**	18.1	84.2	81.8	2.9
		21.0	94.2	91.7	2.7
		23.9	103.9	100.9	2.9
		29.7	122.0	118.2	3.1
		33.2	131.4	127.6	2.9
		38.2	147.4	140.8	4.4

Table F.5: The results of the energy method and experimental data for skewed crossing at 30º.

Type of Bridge	Test Case	Discharge (l/s)	Energy Method Y (mm)	Measured Exp. Data Y (mm)	Errors (%)
AMOSC	**A**	18.1	100.3	108.9	8.6
		21.0	111.6	119.4	7.0
		24.0	121.4	129.9	7.0
		29.8	140.5	150.1	6.9
		33.1	152.0	161.2	6.1
		37.9	175.1	176.9	1.1
AMOSC	**B**	18.1	97.8	107.3	9.7
		21.0	110.0	118.3	7.6
		23.9	120.8	128.4	6.3
		29.7	144.6	148.6	2.8
		33.2	158.4	160.1	1.1
		38.3	181.8	177.5	2.4
AMOSC	**C**	18.1	98.1	108.0	10.1
		21.0	109.8	118.9	8.3
		23.9	119.3	129.5	8.5
		29.7	139.8	149.7	7.1
		33.2	153.2	161.8	5.6
		38.2	177.3	178.5	0.7
ASOE	**A**	18.1	96.7	94.6	2.2
		21.0	106.3	104.8	1.4
		24.0	116.3	115.2	0.9
		29.8	134.4	134.3	0.1
		33.1	147.0	145.1	1.3
		37.9	167.8	160.3	4.4
ASOE	**B**	18.1	92.9	92.8	0.1
		21.0	103.8	103.8	0.0
		23.9	114.3	113.8	0.5
		29.7	137.6	133.5	2.9
		33.2	151.5	145.0	4.3
		38.3	175.5	161.4	8.0
ASOE	**C**	18.1	93.5	93.6	0.1
		21.0	104.3	104.0	0.3
		23.9	113.2	114.4	1.1
		29.7	133.1	132.7	0.3
		33.2	144.6	144.7	0.0
		38.2	167.2	161.2	3.6
DECK	**A**	18.1	96.2	94.2	2.1
		21.0	106.2	104.5	1.6
		24.0	115.9	114.7	1.0
		29.8	133.5	133.2	0.3
		33.1	143.3	143.1	0.1
		37.9	158.2	156.9	0.8
DECK	**B**	18.1	93.5	92.3	1.3
		21.0	103.0	103.1	0.1
		23.9	114.0	113.0	0.9
		29.7	134.7	131.9	2.1
		33.2	147.2	141.8	3.7
		38.3	168.3	156.8	6.8
DECK	**C**	18.1	94.0	93.3	0.7
		21.0	104.3	103.6	0.7
		23.9	113.2	113.6	0.3
		29.7	131.3	132.5	0.9
		33.2	142.2	142.8	0.4
		38.2	158.9	157.4	0.9

Table F.6: The results of the energy method and experimental data for skewed crossing at 45º.

Type of Bridge	Test Case	Discharge (l/s)	Energy Method Y (mm)	Measured Exp. Data Y (mm)	Errors (%)
AMOSC	**A**	18.1	106.4	130.2	22.4
		21.0	116.0	143.0	23.2
		24.0	125.2	155.8	24.5
		29.8	145.2	325.8	124.3
		33.1	157.4	331.0	110.3
		37.9	178.2	339.2	90.4
AMOSC	**B**	18.1	106.8	129.6	21.4
		21.0	117.7	142.6	21.2
		23.9	128.3	154.6	20.5
		29.7	152.8	178.6	16.9
		33.2	169.4	194.9	15.1
		38.3	199.2	249.7	25.3
AMOSC	**C**	18.1	108.2	130.1	20.3
		21.0	118.8	143.3	20.6
		23.9	129.8	155.8	20.0
		29.7	146.8	329.0	124.1
		33.2	159.1	334.4	110.3
		38.2	182.4	343.2	88.2
ASOE	**A**	18.1	101.8	110.0	8.0
		21.0	111.8	122.1	9.2
		24.0	120.4	134.5	11.7
		29.8	140.5	157.0	11.7
		33.1	150.7	169.8	12.7
		37.9	170.4	334.4	96.3
ASOE	**B**	18.1	101.5	109.1	7.5
		21.0	112.0	121.3	8.3
		23.9	123.4	133.4	8.1
		29.7	146.0	156.4	7.1
		33.2	161.2	170.4	5.7
		38.3	187.8	342.9	82.6
ASOE	**C**	18.1	103.2	109.5	6.1
		21.0	113.4	121.7	7.3
		23.9	123.0	133.7	8.7
		29.7	140.0	156.6	11.8
		33.2	153.1	170.1	11.2
		38.2	173.5	340.2	96.1
DECK	**A**	18.1	103.0	109.4	6.2
		21.0	112.6	121.3	7.7
		24.0	120.8	132.8	9.9
		29.8	138.3	154.1	11.4
		33.1	147.4	165.4	12.2
		37.9	162.8	181.6	11.6
DECK	**B**	18.1	102.9	108.7	5.7
		21.0	112.4	120.1	6.8
		23.9	122.9	131.9	7.3
		29.7	143.4	120.1	16.3
		33.2	154.8	165.4	6.8
		38.3	177.2	182.5	3.0
DECK	**C**	18.1	102.8	109.2	6.2
		21.0	112.6	120.8	7.3
		23.9	123.3	132.2	7.2
		29.7	139.8	153.8	10.0
		33.2	150.3	165.3	10.0
		38.2	164.4	182.0	10.7

Vita

Kimia Haji Amou Assar was born in 1994, in Tehran, Iran. She was educated in private schools; she moved to Dubai, United Arab Emirates in 2009 and graduated from Adab Iranian Private High School in 2012. She joined and received a Merit Scholorship at the American University of Sharjah in 2013, from which she graduated as cum laude, in 2016. Her degree was a Bachelor of Science in Civil Engineering.

Ms. Haji Amou Assar began a Master program in Civil Engineering at the American University of Sharjah in 2017. During her graduate studies, she worked for the American University of Sharjah as a Graduate Teaching and Research Assistant in Civil Engineering Department, College of Engineering.